การกำจัดไอออนโลหะจากน้ำเสียโดยใช้คาร์บอนนาโนทิวบ์ที่ดัดแปรด้วยอนุภาคแม่เหล็ก

นายพีรกิตติ์ ธนพิทักษ์

วิทยานิพนธ์นี้เป็นส่วนหนึ่งของการศึกษาตามหลักสูตรปริญญาวิทยาศาสตรมหาบัณฑิต
สาขาวิชาปิโตรเคมีและวิทยาศาสตร์พอลิเมอร์
คณะวิทยาศาสตร์ จุฬาลงกรณ์มหาวิทยาลัย
ปีการศึกษา 2557
ลิขสิทธิ์ของจุฬาลงกรณ์มหาวิทยาลัย

REMOVAL OF METAL IONS FROM WASTEWATER USING MODIFIED MAGNETIC

PARTICLES CARBON NANOTUBES

Mr. Pheerakit Thanapitak

จุฬาลงกรณ์มหาวิทยาลัย
CHULALONGKORN UNIVERSITY

A Thesis Submitted in Partial Fulfillment of the Requirements

for the Degree of Master of Science Program in Petrochemistry and Polymer Science

Faculty of Science

Chulalongkorn University

Academic Year 2014

Thesis Title	REMOVAL OF METAL IONS FROM WASTEWATER USING MODIFIED MAGNETIC PARTICLES CARBON NANOTUBES
By	Mr. Pheerakit Thanapitak
Field of Study	Petrochemistry and Polymer Science
Thesis Advisor	Assistant Professor Fuangfa Unob, Ph.D.

Accepted by the Faculty of Science, Chulalongkorn University in Partial Fulfillment of the Requirements for the Master's Degree

....Dean of the Faculty of Science

(Professor Supot Hannongbua, Dr.rer.nat.)

THESIS COMMITTEE

....Chairman

(Assistant Professor Warinthorn Chavasiri, Ph.D.)

....Thesis Advisor

(Assistant Professor Fuangfa Unob, Ph.D.)

....Examiner

(Associate Professor Nuanphun Chantarasiri, Ph.D.)

....External Examiner

(Assistant Professor Anawat Pinisakul, Ph.D.)

พีรกิตติ์ ธนพิทักษ์ : การกำจัดไอออนโลหะจากน้ำเสียโดยใช้คาร์บอนนาโนทิวบ์ที่ดัดแปร ด้วยอนุภาคแม่เหล็ก (REMOVAL OF METAL IONS FROM WASTEWATER USING MODIFIED MAGNETIC PARTICLES CARBON NANOTUBES) อ.ที่ปรึกษาวิทยานิพนธ์ หลัก: ผศ. ดร.เฟื่องฟ้า อุ่นอบ, 68 หน้า.

ตะกั่วและสังกะสีเป็นไอออนโลหะหนักที่สามารถพบได้ในน้ำเสีย ต้องมีการกำจัดโลหะ เหล่านี้ก่อนปล่อยน้ำออกสู่สิ่งแวดล้อม ในงานวิจัยนี้ ทำการเตรียมตัวดูดซับแม่เหล็กชนิดใหม่โดยการ ใส่อนุภาคแม่เหล็ก Fe_3O_4 ลงบนคาร์บอนนาโนทิวบ์ด้วยวิธีการตกตะกอนร่วม โดยได้ศึกษาปริมาณ อนุภาคแม่เหล็กที่เติมลงไปในช่วง 20 ถึง 30 %โดยน้ำหนัก จากนั้นดัดแปรคอมพอสิตแม่เหล็กด้วย สารละลาย 8-ไฮดรอกซีควิโนลีน ทำการพิสูจน์เอกลักษณ์คอมพอสิตด้วยการส่องกล้องจุลทรรศน์แบบ ส่องกราด TGA และ FT-IR ผลการทดลองแสดงว่าผิวของคาร์บอนนาโนทิวป์ถูกปกคลุมด้วยอนุภาค แม่เหล็กและ 8-ไฮดรอกซีควิโนลีน ความเป็นแม่เหล็กของคอมพอสิตที่ตรวจสอบด้วยเครื่องมือ VSM พบว่า MWCNT-25Mag-8-HQ และ MWCNT-30Mag-8-HQ แสดงค่าความเป็นแม่เหล็กที่ 6.726 emu/g และ 8.137 emu/g ตามลำดับ ส่วนของ MWCNT-25Mag และ MWCNT-30Mag แสดงค่าความเป็นแม่เหล็กที่ 15.819 emu/g และ 19.907 emu/g ตามลำดับ เวลาในการถึงจุด สมดุลของกระบวนการดูดซับคือ 60 นาที และค่า pH ที่เหมาะสมสำหรับกระบวนการนี้คือ 5 โดย adsorption kinetics เป็นไปตาม pseudo-second order model และ adsorption equilibrium สามารถอธิบายได้ด้วย Langmuir isotherm ความสามารถในการดูดซับไอออนตะกั่วสูงสุดของ MWCNT-30Mag และ MWCNT-30Mag-8-HQ คือ 32.26 mg/g และ 48.78 mg/g ตามลำดับ และ ดูดซับไอออนสังกะสีสูงสุดได้ 12.22 และ 18.52 mg/g ตามลำดับ

สาขาวิชา   ปิโตรเคมีและวิทยาศาสตร์พอลิเมอร์ ลายมือชื่อนิสิต _____

ปีการศึกษา 2557   ลายมือชื่อ อ.ที่ปรึกษาหลัก _____

5472059723 : MAJOR PETROCHEMISTRY AND POLYMER SCIENCE

KEYWORDS:

PHEERAKIT THANAPITAK: REMOVAL OF METAL IONS FROM WASTEWATER USING MODIFIED MAGNETIC PARTICLES CARBON NANOTUBES. ADVISOR: ASST. PROF. FUANGFA UNOB, Ph.D., 68 pp.

Lead and zinc could be found in wastewater. In order to treat the wastewater before its release to the environmental source, these heavy metals have to be removed. In this work, a new magnetic adsorbent was prepared by loading the Fe_3O_4 magnetic particles onto carbon nanotubes through co-precipitation method. The amount of Fe_3O_4 magnetic particles was varied from 20 to 30%wt. The magnetic composite was further modified with 8-hydroxyquinoline solution. The composites were characterized by SEM, TGA and FT-IR. The results showed that the surface of carbon nanotubes was covered by magnetic particles and 8-hydroxyquinoline. The VSM results showed that the adsorbents with 25% and 30% wt magnetic particles and 8-hydroxyquinoline had the magnetization value of 6.726 emu/g and 8.137 emu/g, respectively and the adsorbents that contain only 25% and 30% wt magnetic particles were 15.819 emu/g and 19.907 emu/g, respectively. The composite of MWCNT and magnetic particles with 8-HQ and without 8-HQ (MWCNT-Mag and MWCNT-Mag-8-HQ) were used as adsorbents for Pb(II) and Zn(II) ions adsorption. The time for the adsorption process to reach the equilibrium was 60 minutes and the suitable pH value for metal ions adsorption was pH 5. The adsorption kinetics followed pseudo-second order model and the adsorption equilibrium could be described by Langmuir isotherm. The maximum capacity of MWCNT-30Mag and MWCNT-30Mag-8-HQ in Pb(II) adsorption was 32.26 mg/g and 48.78, respectively. On the other hand, the maximum capacity of MWCNT-Mag and MWCNT-Mag-8-HQ in Zn(II) adsorption was 12.22 and 18.52 mg/g , respectively

Field of Study: Petrochemistry and   Student's Signature _____
                  Polymer Science   Advisor's Signature _____
Academic Year: 2014

ACKNOWLEDGEMENTS

CONTENTS

LIST OF TABLES

LIST OF FIGURES

LIST OF ABBREVIATIONS

8-HQ	8-hydroxyquinoline
cm^{-1}	wave number unit
FAAS	flame atomic absorption spectrometer
FT-IR	fourier transform infrared spectrometer
g	gram
hr	hour
ICP-OES	inductively coupled plasma-optical emission spectrometer
L	liter
nm	nanometer
M	molar
Mag	magnetic particles
mg	milligram
min	minute
μL	microliter
MWCNT	multi-walled carbon nanotube
ppm	part per million/milligram per liter
SEM	scanning electron microscope
TGA	thermo gravimetric analysis
VSM	Vibrating sample magnetometer
XRD	X-ray diffractometer

CHAPTER I

INTRODUCTION

1.1 Statement of the problem

Heavy metals are one of the most important components which were side products from many industries. Many heavy metals in waste could be harmful to the environment and human if they are not removed by suitable treatment process. Thus, the removal or reduction of the amount of these metal ions from wastewater before its reuse is a requirement. There are a number of processes used for purification, for wastewater treatment was normally use coagulation, oxidization of sulfuric acid and vacuum distillation, extraction and adsorption. One of the most widely used and interested methods for removal heavy metal ions is adsorption process because of its simplicity and low cost [1]. Thus, it was the interested idea for our adsorbent.

Carbon nanotubes are widely used as an adsorbent and supporter due to its high surface area and the simplicity of its regeneration by heat treatment [2, 3]. There is some research using carbon nanotubes as a support for coating magnetic particles to removal organic substances [4-6]. Magnetic separation has become a widely used process for adsorption because of its simply and quickly process. It has been used for many applications in biochemistry, analytical chemistry and mining ores [7]. The mainly advantage of this technology is that the magnetic separation can be easily collected using only external magnetic field [8]. The ferric oxide (Fe_3O_4) is one of magnetic particles that widely used to apply the magnetism for adsorbent due to it easily to generate and no effect to the environment with good electromagnetic performance. The poor thing of magnetic particles was their aggregation that effect to decrease the ability to disperse in water so it may lead to a reduction in removal efficiency. In this research, carbon nanotubes are used as the support for iron oxide (magnetite) particles and 8-hydroxyquinoline to reduce the aggregation of magnetic particles. The iron oxide – carbon nanotubes – 8-hydroxyquinoline composite was used for removal of zinc and lead ions from aqueous solutions.

8-hydroxyquinoline (8-HQ) is also known as 8-quinolinol and usually used as a chelating agent in analytical chemistry due to its ability to form complex with metal ions. Its molecule bares an oxygen donor atom and nitrogen donor atom and both atoms bind to metal atoms [9, 10]. Its ability to form complexes with metal ions is expected for an increase in selectivity of composites in adsorption of heavy metal ions.

1.2 Objective of this work

To synthesize a composite of magnetic particles-activated carbon-8-hydroxyquinoline and to investigate its properties in heavy metal ions adsorption under influence of various parameters.

1.3 Scope of this work

This research was started with the synthesis of the composite between activated carbon and ferric oxide by co-precipitation method. Then, the products from previous step were characterized using X-ray diffraction (XRD), scanning electron microscope (SEM) and fourier transform infrared spectrometer (FTIR).The composites were further modified with 8-hydroxyquinoline and characterized by Fourier transform infrared spectrometer (FTIR). The factors (adsorption time and pH value) that affected on adsorption efficiency were investigated with batch method and the kinetics and isotherms of adsorption were also studied in aqueous solutions. Final step, the adsorbents efficiency in removal of heavy metal ions (Zinc and lead) from waste lubricant will be investigated.

1.4 The benefits of this works

To obtain new magnetic composites that has ability to remove heavy metal ions from water and waste lubricant.

CHAPTER II

THEORY AND LITERATURE REVIEWS

2.1 Magnetic materials

In most atoms, electrons exist in pairs. Electrons in each pair spin in opposite directions. Hence, when electrons are paired together, their opposite spins cause their magnetic fields to cancel each other and there is no net magnetic field. On the other hand, materials having some unpaired electrons will have a net magnetic field and react more to an external magnetic field [11-13].
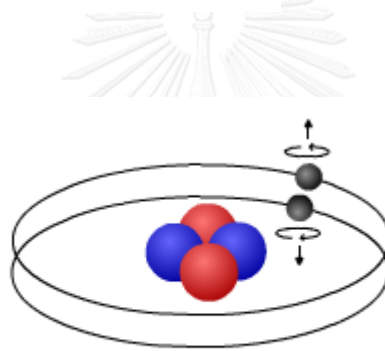
Figure 2.1 The opposite spins of electron pair where grey balls are electrons, red balls are protons and blue balls are neutrons [11].

Magnetic materials can be classified from how they respond to magnetic fields. There are three main classifications of magnetic materials which are diamagnetic, paramagnetic and ferromagnetic.

2.1.1 Diamagnetic materials

In diamagnetic materials, all electrons are paired and therefore, there is no permanent net magnetic moment per atom. Diamagnetic materials have a weak, negative susceptibility to magnetic fields. They are slightly repelled by a magnetic field and the material does not retain the magnetic properties if there are no external magnetic fields. Diamagnetic properties are the results of the realignment

of the electron paths when there is the influence of an external magnetic field. Most elements in the periodic table e.g. copper, silver, and gold, are diamagnetic.

2.1.2 Paramagnetic materials

Paramagnetic materials will be weakly affected by external magnetic fields due to the presence of some unpaired electrons and the realignment of the electron paths caused by the external magnetic fields. However, these materials do not retain the magnetic properties if there are no external magnetic fields. Paramagnetic materials include magnesium, molybdenum, lithium, and tantalum.

2.1.3 Ferromagnetic materials

In ferromagnetic materials, their atoms have some unpaired electrons and therefore a net magnetic moment. Ferromagnetic materials have a positive susceptibility to an external magnetic field. They are strongly attracted to magnetic fields and also able to retain their magnetic properties although there are no external magnetic fields. Their strong magnetic properties arise from the alignment of atomic moments. Ferromagnetic materials include iron, nickel, and cobalt.

2.2 Iron oxides

Iron oxides are ferromagnetic materials. Iron (II, III) oxides with formula Fe_3O_4 (magnetite) is one of a number of iron oxides, the others are iron (II) oxide (FeO) and iron (III) oxide (Fe_2O_3) called hematite. Iron (II, III) oxide occurs in nature as the mineral magnetite that contains both Fe^{2+} and Fe^{3+} ions [14].

2.2.1 Magnetite (Fe_3O_4)

Magnetite is one of the three main oxides of iron. These magnetic materials have been widely investigated because of their magnetic properties and also non-toxic and biocompatible properties. The crystalline structure of magnetite is cubic inverse spinal (Figure 2.2) [11, 15, 16].
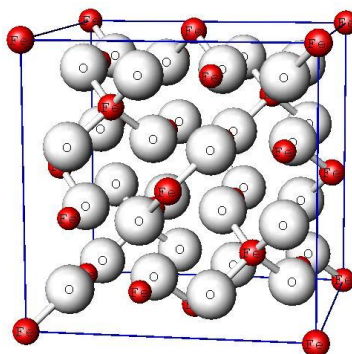
Figure 2.2 Crystal structure of Iron (II, III) oxide (magnetite). Red and white balls are iron atoms and oxygen atoms.

2.3 Synthesis of magnetite

There are several methods for magnetite synthesis. Some of methods are described briefly as follows.

2.3.1 Chemical co-precipitation method

The chemical co-precipitation method is one of the most used processes for producing magnetic materials due to its simple and quick process. Iron (II) solution (from iron (II) chloride or iron (II) sulfate) is mixed with iron (III) solution (from iron (III) chloride or iron (III) sulfate) as staring mixture solution. Then, alkaline solution (NaOH or NH_4OH) is dropped into the solution as the precipitating agent. The reaction is shown in equation (2.1) [17-19].

$$Fe^{2+} + 2Fe^{3+} + 8OH^- \longrightarrow Fe_3O_4 + 4H_2O \qquad (2.1)$$

2.3.2 Reverse co-precipitation method

The reverse co-precipitation method is an opposite process compared to ordinary chemical co-precipitation. In this method, the iron salts containing Fe(II) and Fe(III) are dissolved and mixed together. Then, iron salt mixture was slowly dropped into an alkaline solution. The whole procedure is schematically presented in Figure 2.3.
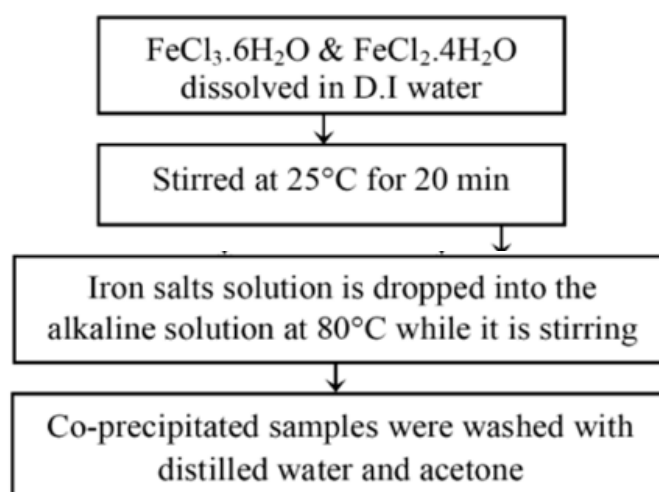
Figure 2.3 Process of reverse co-precipitation [20].

2.3.3 Oxidation-precipitation method

In the oxidation-precipitation method, iron salt was mixed with de-ionized water, monoethanolamine (MEA) and H_2O_2 with a pump. Pumping rate must not be too fast. After the appropriate time, the black precipitants (magnetite) occurred [21].

2.3.4 Reduction of mineral magnetite method

The reduction of mineral was started by mixing sodium hydroxide solution and oleic acid in a three-neck round-bottom flask. Mineral magnetite was dissolved in hydrochloric acid under mechanical stirring and grey precipitates were formed. The solution of ferrous–ferric ions is filtered with a fritted funnel and added into three-neck round-bottom flask dropwise under constant stirring. After that, separated magnetically and gain the black solid (magnetite) [22].

2.3.5 Sol-gel method

In this method, ferric nitrate is dissolved in ethylene glycol under continuous stirring and heating at $40^{\circ}C$ for 2 hours to generate "sol". Then, the sol is heated up to $80^{\circ}C$ for a moment and "gel" is produced. After that, gel is dried in an oven and becomes "xerogel" that is further annealed in the temperature range of

200 to 400°C under vacuum. Finally, the magnetic nanoparticles with the different size are obtained [23, 24].

Fe(NO$_3$)$_3$ + HOCH$_2$CH$_2$OH $\rightarrow$ Sol $\longrightarrow$ Gel $\longrightarrow$ Xerogel $\longrightarrow$ annealed under vacuum $\longrightarrow$ Fe$_3$O$_4$
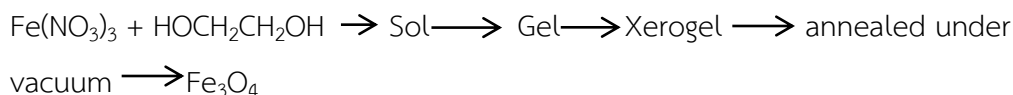
Figure 2.4 The procedure of synthesizing magnetic nanoparticles.

2.3.6 Microemulsion method

In the microemulsion method, the surfactant aqueous solution is mixed with oil phase such as n-heptane and n-hexanol under argon atmosphere and low heating. An aqueous iron(II) sulfate solution is rapidly added into the mixture and an aqueous ferric chloride solution is subsequently added. Then, an emulsion consisted of ammonia in aqueous solution of the same surfactant and an oil phase is added dropwise under argon atmosphere and vigorous stirring. The obtained product is repeatedly washed with ethanol and deionized water. Finally, magnetic nanoparticles are dried in an oven.
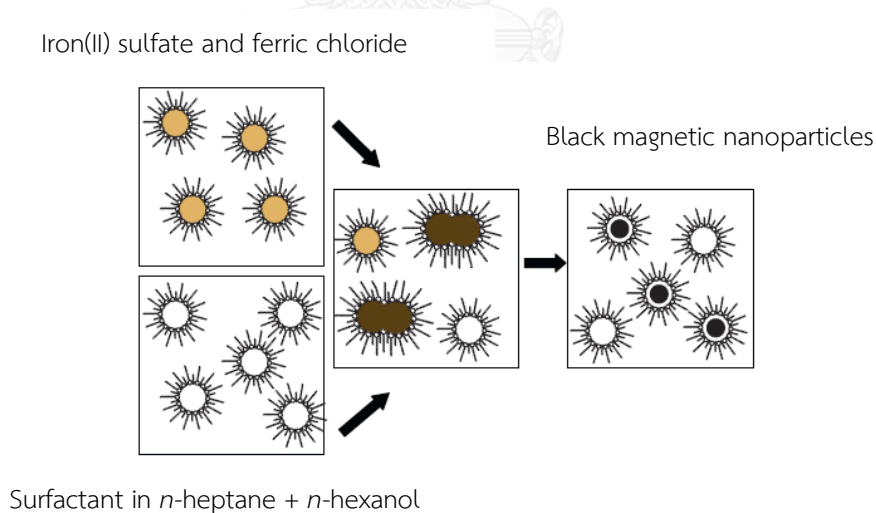
Figure 2.5 Mechanism of the formation of magnetic nanoparticles [25].

2.4 Carbon nanotubes

Carbon nanotubes (CNTs) are tube-shaped material that is made from carbon with diameter in nanometer scale. The size of CNTs diameter is in a range between

1- 50 nm. They exhibit many good properties such as thermal resistance, chemical resistance and high surface area. They are categorized by structure into two types which are single-walled nanotube (SWNT) and multi-walled nanotubes (MWNT).

- Single-walled nanotubes (SWNT) are tubes of graphite that have a single layer cylindrical wall of graphite, called graphene that rolls into a seamless tube. Most of SWNTs have diameter approximately 1 nm but their length ranges from millimeter to centimeter scale [26, 27].
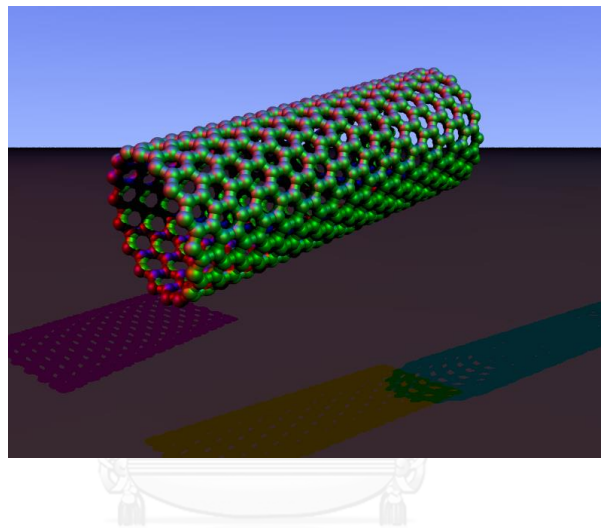
Figure 2.6 Single-walled carbon nanotubes (SWCNTs).

- Multi-walled nanotubes (MWNTs) consist of many layers of graphene. A single sheet of graphite is rolled around as inside layer and repeatedly rolled like this to form multi-layer nanotube. The diameter of MWNTs is normally in the range of 5-50 nm [26, 27].
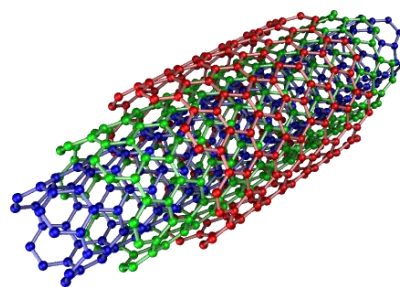
Figure 2.7 Multi-walled carbon nanotubes (MWCNTs).

Multi-walled carbon nanotubes are used in various fields. Due to its highly surface area, they have been widely used as adsorbents for metal ions adsorption or gas adsorption. The efficiency is up to their pore size. Their surface chemical modification is often performed in order to obtain the surface properties that suit their use.

2.5 Information of metal ions, zinc and lead

2.5.1 Zinc

Zinc and their compounds are used in many industrials such as using as an anti-corrosion, alloy, rubber, paints, cosmetics, pharmaceuticals, and in batteries industrials. Commercially, zinc is obtained from its ores (mainly gained by mining) by concentrating and roasting the ore, then reducing the previous composite (zinc, silver and lead) to zinc thermally with carbon or by electrolysis [28].

2.5.2 Lead

Lead is present in the lead-zinc-silver ore in the higher concentrations than silver and zinc. After the processing of the ore, higher amount of lead will be obtained per pound of ore, compared to zinc and silver. The application for lead and its compounds in industrial can be divided into two groups [29].

2.5.2.1 Inorganic lead component

Metallic lead was mixed with some other metal or alloys or solder to form plate sheet or wire in chemical industry and filter in electronics industry. Oxide of lead is used in paint and battery industries. Salts of lead have various colors and therefore they are used as primary color pigment in paint industry such as yellow color from lead chromate, white color from lead carbonate. Lead acetate is used in cosmetic industry and lead nitrate in plastic and rubber industries.

2.5.2.2 Organic lead component

Tetraethyl lead and tetramethyl lead were mixed with benzene fuel to increase octane number. Compared with inorganic lead components, organic lead components are much more toxic because they are easily

spread to the surroundings by exhaustion from pipe. Hence they now stop using organic lead compounds in the fuel field.

2.6 Treatment of heavy metals in wastewater

There are several treatment techniques to remove heavy metal ions from wastewater. The methods are briefly described as follows [30].

2.6.1 Chemical precipitation

The chemical precipitation technique converts soluble metal ions to insoluble forms (solid) that can be separated from solution. Various chemicals are used as precipitants but the most commonly used methods are hydroxide precipitation and sulfide precipitation. This method is divided into two steps. First, precipitants are mixed with metal ions in water and precipitation occurs. The second step is the separation of solid by filtration or flocculation.

2.6.1.1 Hydroxide precipitation

This method is the most widely used because of their convenience and low cost. The chemicals that are used as precipitants include lime ($Ca(OH)_2$) and caustic soda ($NaOH$). The precipitation would occur in specific range of pH value. The reactions of precipitation are shown in equations 2.1 and 2.2.

$$M^{2+}_{(aq)} + Ca(OH)_{2(aq)} \longrightarrow M(OH)_{2(s)} \downarrow + Ca^{2+} \tag{2.1}$$

$$M^{2+}_{(aq)} + 2NaOH_{(aq)} \longrightarrow M(OH)_{2\,(s)} \downarrow + 2Na^{+} \tag{2.2}$$
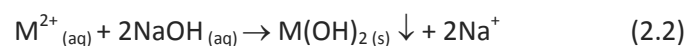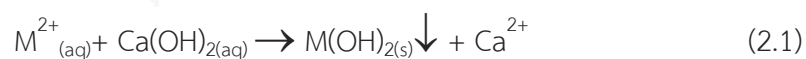
Lime is used more often than caustic soda. It is cheaper in cost than caustic soda but it produces a larger volume of sludge than caustic soda.

2.6.1.2 Sulfide precipitation

Sulfide precipitation is one of the most commonly used methods like hydroxide precipitation. The advantage of this process over hydroxide precipitation is the ability to reduce hexavalent chromium to its trivalent state. There

are two most common processes for sulfide precipitation which are the soluble sulfide process and the insoluble sulfide (Sulfex) process.

2.6.1.2.1 Soluble sulfide process

Sodium sulfide as a liquid reagent is used in this process. The soluble sulfide results in a rapid precipitation of metal ions. The generated particles are fine precipitate particles and hydrated colloidal particles. Because the particles size is very small, so they do not settle well. The coagulating and flocculating agents are added to induce the formation of bigger size particles for faster settling. The reaction of soluble sulfide is shown in equation 2.3.

$$M^{2+}_{(aq)} + Na_2S_{(aq)} \longrightarrow MS_{(s)} \downarrow + 2Na^+ \qquad (2.3)$$

In soluble sulfide process, high concentration of soluble sulfide is applied in order to generate hydrogen sulfide gas (H_2S). The dosage must be controlled strictly.

2.6.1.2.2 Insoluble sulfide process (Sulfex)

The insoluble sulfide process starts with the addition of ferrous sulfide (FeS) into water that contains dissolved metal and metal hydroxide. Then, FeS will disassociate into ferrous and sulfide ions. Sulfide ions are consumed in the precipitation of the metal pollutants and ferrous ions will precipitate as iron hydroxide. The reactions are shown in equations 2.4.-2.7.

$$FeS_{(aq)} \longrightarrow Fe^{2+}_{(aq)} + S^{2-}_{(aq)} \qquad (2.4)$$

$$M^{2+}_{(aq)} + S^{2-}_{(aq)} \longrightarrow MS_{(s)} \downarrow \qquad (2.5)$$

$$M(OH)_{2\,(aq)} \longrightarrow M^{2+}_{(aq)} + 2(OH)^-_{(aq)} \qquad (2.6)$$

$$Fe^{2+}_{(aq)} + 2(OH)^-_{(aq)} \longrightarrow Fe(OH)_{2\,(s)} \downarrow \qquad (2.7)$$
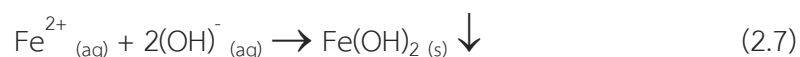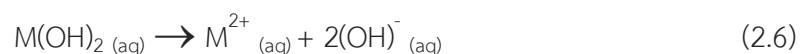
The advantage of insoluble sulfide process is that it does not generate hydrogen sulfide gas. However, it produces higher amount of sludge, compared to hydroxide or soluble sulfide process.

2.6.2 Membrane filtration

Membrane filtration systems are processes which semi-permeable membranes and pressure differential are employed to remove solids in waste streams. Reverse osmosis and ultrafiltration are two commonly used membrane filtration processes.

2.6.2.1 Ultrafiltration

Ultrafiltration was used for metal-finishing wastewater and oily wastes. It can remove substances with molecular weights greater than 500 such as large organic molecules and heavy metals. It can be used when the size of solute molecules are ten times greater than the size of the solvent molecules. A semi-permeable microporous membrane performs the separation. Wastewater is passed through membrane modules under pressure. Water and low molecular weight solutes (e.g. salts and some surfactants) will pass through the membrane and are removed as permeate.

2.6.2.2 Reverse osmosis

Reverse osmosis (RO) is a process for separating dissolved solids from water. RO is commonly used for treating oily or metal-bearing wastewater. RO is working under condition where the solute molecules are approximately in the same size as the solvent molecules. The separation occurs by aid of a semi–permeable, microporous membrane and pressure. This method is effective in removing dissolved metals.

2.6.3 Ion exchange

This is a process for removal of heavy metals ions from relatively low–concentration waste streams. The wastewater stream is passed through a resin media bed. Resin contains bonded groups having ionic charge on the surface with counter ions that will be exchanged by ions of the same charge in wastewater. There are cationic and anionic class of resins for specific usage depending on the contaminants to be removed. The advantages of this process are that it can remove the metal ions

and then recover for further reuse. However, the resins could be fouled after using for a while. Then, it has to be regenerated or changed to a new one.

2.6.4 Electrolytic recovery

In the electrolytic recovery process, oxidation and reduction reactions take place. The conductive electrodes (anodes and cathodes) are immersed in the metal wastewater and an electric potential is applied. At the cathode, metal cations are reduced to its elemental form (electron-consuming reaction). At the same time, gases such as oxygen, hydrogen, or nitrogen were generated from the oxidation reaction at the anode (electron-producing reaction). After the metal coating on the cathode reaches a desired thickness, it may be removed and recovered. This process is not widely used due to their high cost in operation. The reactions are shown in Figure 2.8.
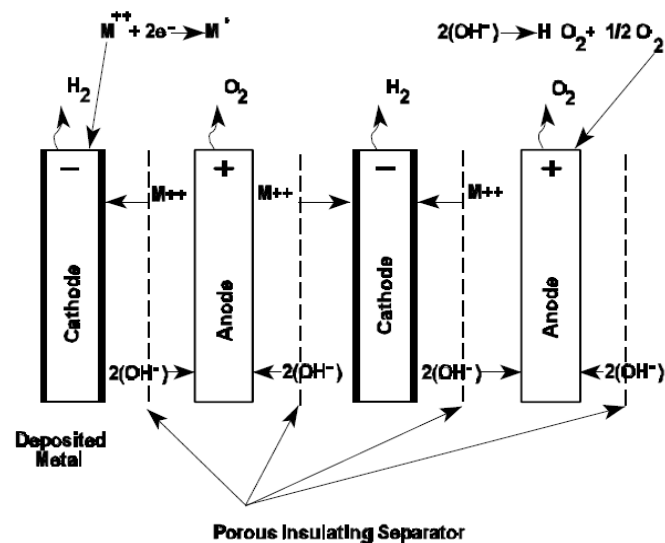
Figure 2.8 Electrolytic system diagram for metal recovery [30].

2.6.5 Carbon Adsorption

Activated carbon is used as an adsorbent for removal of dissolved contaminants from wastewater. The wastewater stream comes in contact with activated carbon and the contaminants are adsorbed onto the surface of activated carbon. After being used for a certain period of time, phenomenon called

breakthrough would occur from activated carbon column. This phenomenon is the results of the saturation of active site capacity of activated carbon or column exhaustion. At this point, the effluent pollutant concentration increased. After the carbon is exhausted, it should be removed and regenerated. The process diagram is shown in Figure 2.9.
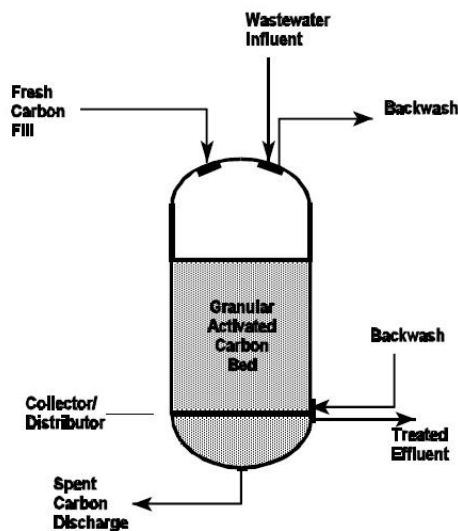
Figure 2.9 Carbon adsorption system diagram [30].

2.7 Adsorption

Adsorption is the process of the mass transfer of adsorbates in gas or liquid phase to the adsorbent surface. Adsorption can be divided into two groups which are physisorption and chemisorption that will be described in the following sections [31].

2.7.1 Adsorption process

Adsorption process involves the mass transfer of analytes and different steps in adsorption are proposed as shown in Figure 2.10.
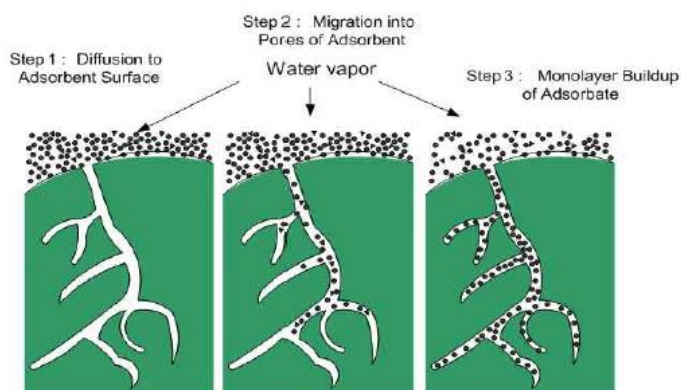
Figure 2.10 The steps of adsorption onto the adsorbent surface [31].

2.7.1.1 Bulk transport

This step is very fast. The analytes will diffuse from bulk solution to the surface of boundary layer or the layer of solvent on adsorbent surface.

2.7.1.2 Film transport

This step will occur slowly. The analytes will diffuse through the boundary layer and move on to the surface of adsorbent. This step is called film diffusion or external diffusion.

2.7.1.3 Intraparticle transport

This step is often the rate determining step of adsorption. The analytes move from the adsorbent surface to inside or into the pore of adsorbent and/or react with the active sites. This step is also called internal diffusion.

2.7.2 Physisorption

In physical adsorption, the forces of attraction between the molecules of adsorbate and the adsorbent are weak such as van der Waals force or electrostatic interaction without forming chemical bond. Multilayer sorption can occur on the adsorbent surface when the concentration of the adsorbate in bulk solution is increased. Since the forces of attraction are weak, the process of physisorption can be easily reversed by heating or decreasing the pressure (as in the

case of gases) or concentration of the adsorbate. Monolayer and multilayer sorption are shown in Figure 2.11.
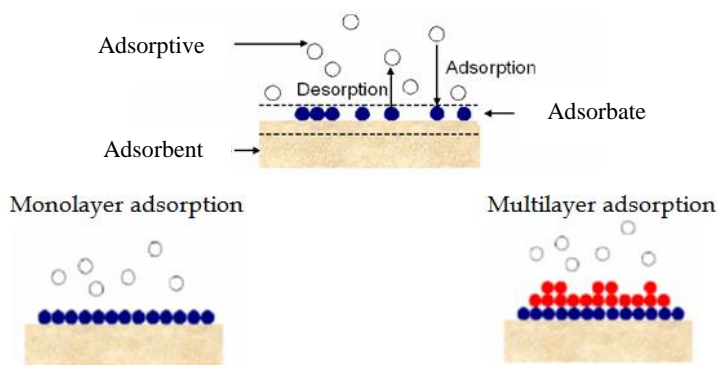
Figure 2.11 Monolayer and multilayer sorption [32].

2.7.3 Chemisorption

In chemisorption, the forces of attraction between the adsorbate and the adsorbent are strong due to the chemical bond formation which is stronger than the interaction force that appears in physisorption. This process is more specific to the certain groups of analytes due to the interaction with specific active site on the adsorbent. Thus, this process is irreversible and monolayer of adsorbates on surface is generally formed.

Table2.1 Comparison between physisorption and chemisorption

Physisorption	Chemisorption
Force of attraction are van der Waals forces.	Force of attraction are chemical bond formation.
This process is observed under conditions of low temperature.	This process takes place at high temperatures.
It is not spectfic.	It is highly specific.
Low enthalpy of adsorption.	High enthalpy of adsorption
Multi-molecular layer may be formed.	Generally, mono-molecular layer is formed.
This process is reversible.	This process is irreversible.

2.8 Adsorption isotherms

Adsorption isotherms are fundamental in describing equilibrium of the analytes adsorption onto adsorbent surface. The adsorption isotherm expresses the relation between the amount of analyte adsorbed on adsorbent and concentration of analytes in solution at equilibrium. The experimental data are often fitted to widely used adsorption isotherm models such as Langmuir and Freundlich [33].

2.8.1 Langmuir isotherm

The assumption of Langmuir model is based on the adsorption that takes place at specific and homogeneous sites on the adsorbent. The adsorption is in monolayer regime and the maximum adsorption capacity at equilibrium can be predicted. The energy of adsorption onto the adsorbent surface is constant. The Langmuir isotherm equation is written in equations 2.8.

$$q_e = \frac{q_m b C_e}{1 + b C_e} \qquad (2.8)$$

Langmuir isotherm in equation 2.8 can be linearized to equation 2.9;

$$\frac{C_e}{q_e} = \frac{1}{b q_m} + \frac{C_e}{q_m} \qquad (2.9)$$

where q_e = the amount of solute adsorbed per unit weight of adsorbent at equilibrium (mg/g)

q_m = maximum adsorption capacity for forming single layer (mg/g)

b = the constant related to the free energy of adsorption (L/mg)

C_e = the equilibrium concentration of the solute in the bulk solution (mg/L)

A plot of C_e/q_e versus C_e should give a straight line with intercept of $1/bq_m$ and slope of $1/q_m$ as shown in Figure 2.12 [30].
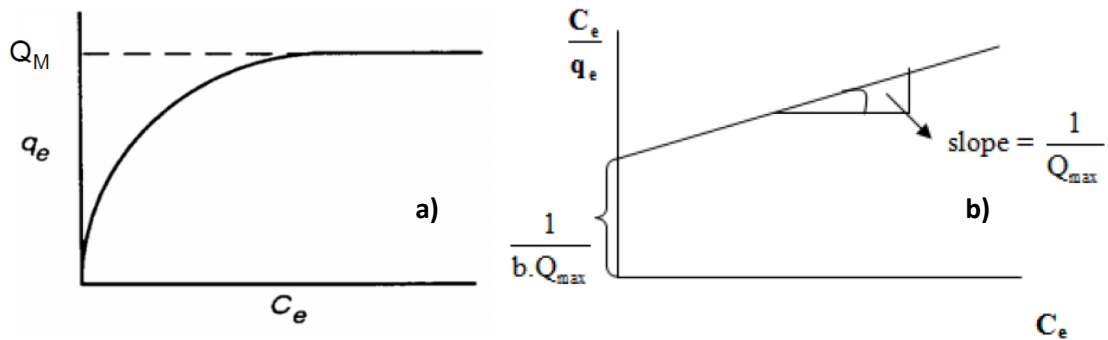
Figure 2.12 The isotherm shape (a) and linear plot (b) of Langmuir adsorption.

2.8.2 Freundlich isotherm

The Freundlich isotherm model was derived by assuming that the adsorption of analytes occurred on heterogeneous surface or on active sites of various affinities. The Freundlich model equation is shown in equation 2.10.

$$q_e = K_f\, C_e^{1/n} \qquad\qquad (2.10)$$

1/n is a measure of intensity of adsorption. The higher the 1/n value, the more favorable the adsorption is ($n < 1$ or $\dfrac{1}{n} > 1$)

The Freundlich expression is an exponential equation. The equation can be linearlized with logarithmic form as presented in equation 2.11;

$$log q_e = log K_f + \tfrac{1}{n} log C_e \qquad\qquad (2.11)$$

where K_f = Fruendlich constant, an indicator of adsorption capacity of the adsorbent (mg/g).

   1/n   = a measure of intensity of adsorption.

A plot of log q_e versus log C_e should give a straight line with intercept of log K_f and slope of 1/n as shown in Figure 2.13
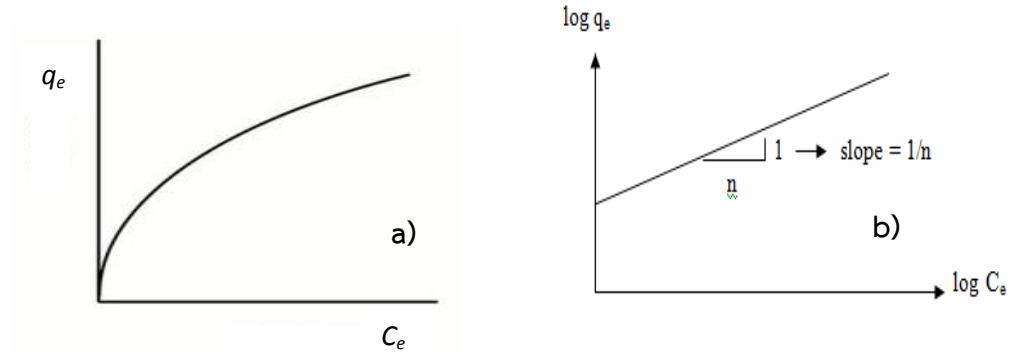
Figure 2.13 The isotherm shape (a) and linear plot (b) of Freundlich adsorption [30].

2.9 Literature review

There are many investigations about the removal of pollutants from wastewater by adsorption. Various adsorbents were developed, the results and improvement has been reported.

Among many adsorbents, the magnetic composite material is one of the most interesting materials in the field. There are some researchers that used magnetic composite to remove metal ions or contaminant from water or solutions as summarized in Table 2.2. Magnetic composite can be separated easily from water by only applying external magnetic field

Table2.2 The adsorption capacity of various magnetic composite in contaminant adsorption

Adsorbents	Contaminants	Adsorption condition			Ref.
		pH	time(min)	Adsorption capacity(mg/g)	
Guar gum-MWCNT-Fe_3O_4	Neutral red	-	120	28.36	[6]
	Methylene blue			37.17	
Co-Fe_2O_4-Activated carbon	Malachite green	5	20	49.21	[7]
Fe_2O_3-MWCNT	Methyl orange	3		≈ 28	[34]
		4		≈ 38	
		5	10	≈ 35	
		6		≈ 34	
		7		≈ 25	
Fe_3O_4-MWCNT	Neutral red	7	360	9.77	[35]
	Methylene blue			11.86	
	brilliant cresyl blue			6.28	
Al_2O_3-Fe_3O_4	Cd^{2+}	6	240	625	[36]
Fe_3O_4-SiO_2	Zn^{2+}	6	100	119	[16]

In this work, we are interested in the use of Fe_3O_4 magnetic particles and modified with 8-hydroxyquinoline supported by MWCNT (MWCNT-Mag-8-HQ) for removal heavy metal ions.

MWCNT-Mag-8-HQ has both magnetic performance from Fe_3O_4 and ability to form complex with heavy metal ions due to the presence of 8-HQ. The parameters that could affect to the adsorption were studied.

CHAPTER III

EXPERIMENTALS

3.1 Chemicals and instruments

3.1.1 Chemicals

All reagents in the experiments are shown in Table 3.1. The chemicals were of analytical grade and were used as received without further purification.

Table3.1 Chemical

Chemicals	Distributor
Sodium hydroxide	Emsure
Ammonium ferrous sulfate	Allied Chemical
Ammonium ferric sulfate	Baker Analyzed
Nitric acid 65% w/w	Emsure
Sodium nitrate	Fluka
Ammonia solution	Emsure
Ethanol	Emsure
Multi-walled carbon nanotubes	Smart Materials
Lead ions standard solution (1000 mg/L)	Ajax Finechem
Zinc ions standard solution (1000 mg/L)	Ajax Finechem
Iron(III) ions standard solution (1000 mg/L)	Ajax Finechem
8-Hydroxyquinoline	Himedia

3.1.2 Instruments

All instruments used in all experiments are listed in Table 3.2.

Table3.2 List of instruments

Instruments	Model
pH meter	Mettler Toledo/S220
Thermogravimetric analysis (TGA)	Pyris 1
X-ray diffractometer (XRD)	Bruker AXS/Diffraktometer D8
Scanning electron microscope (SEM)	Jeol/JSM 5800
Fourier transform infrared spectrometer (FT-IR)	Nicolet/6700
Flame atomic absorption spectrometer (FAAS)	AAnalyst100 (Perkin Elmer)
Inductively coupled plasma-optical emission	Thermo/iCAP 6000 Series
Vibrating Sample Magnetometer (VSM)	LakeShore/7404

3.2 Synthesis of the composite of multi-walled carbon nanotubes, magnetic nanoparticles (Fe$_3$O$_4$) and 8-hydroxyquinoline

The composite synthesis was divided into two steps as described as follows.

3.2.1 Synthesis of the multi-walled carbon nanotubes and magnetic nanoparticles (Fe$_3$O$_4$) composite (MWCNT-Mag)

The method in this research was adapted from the co-precipitation method proposed by Gong et al [37]. A solution of ferrous ions and ferric ions were prepared by dissolving 0.170, 0.213 or 0.258 g ammonium ferrous sulfate in 20 ml of deionized water and 0.417, 0.521 or 0.630 g ammonium ferric sulfate in 80ml of deionized water under electromagnetic stirring, respectively. Then, two iron solutions with Fe(II):Fe(III) mole ratio of 1:2 were mixed together and heated up to 80 $^\circ$C. A portion of 0.500 g multi-walled carbon nanotubes was added into the mixed iron solution under continuous stirring. After that, a solution of 5M ammonium hydroxide was added dropwise into the mixture. The mixture was let stand for 5 minutes for

the co-precipitation of magnetic nanoparticles on multi-walled carbon nanotubes surface to occur.
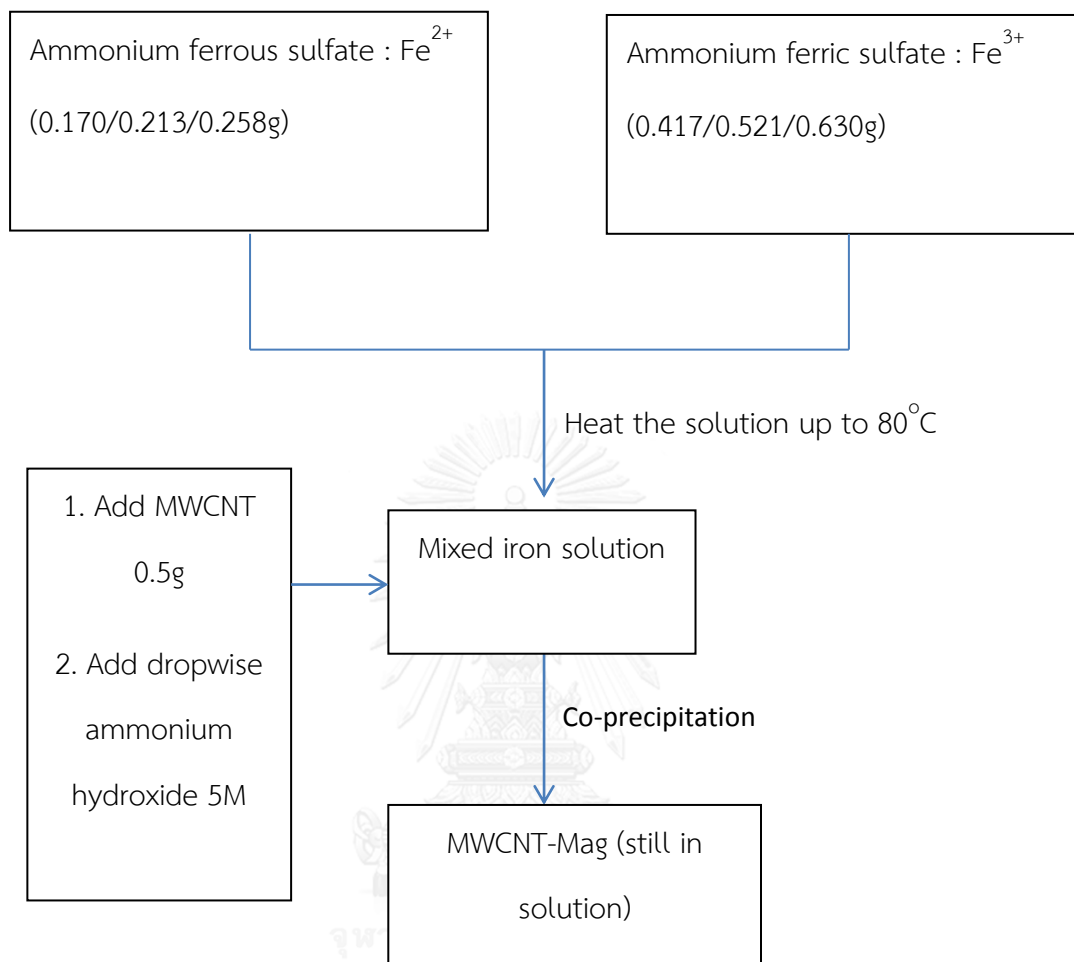
Figure3.1 Procedure of MWCNT-Mag synthesis

3.2.2 Synthesis of 8-hydroxyquinoline doped MWCNT-Mag (MWCNT-Mag-8-HQ)

Immediately after MWCNT-Mag was obtained, a solution of 8-hydroxyquinoline (0.300g in 10ml of ethanol) was added dropwise at 80°C under continuous stirring for 30 minutes. Then, the mixture was stirred at room temperature for another 5 hours. Finally, the obtained composite (MWCNT-Mag-8-HQ) was separated out by using external magnet and washed with deionized water and ethanol, respectively. The solid was dried in an oven at 80°C for 24 hours.

```
┌─────────────────────────────────────┐
│      MWCNT-Mag (in the mixture)      │
└─────────────────────────────────────┘
┌──────────────────┐  Add dropwise
│  8-HQ in ethanol │  ─────────►
└──────────────────┘
┌─────────────────────────────────────┐
│         MWCNT-Mag-8-HQ               │
└─────────────────────────────────────┘
```

┌──────────────────────────────────────┐
│ 1. Stop heating.   │
│ 2. Stir the mixture continuously for │
│ 5 hours.   │
│ 3. Wash the solid with deionized   │
│ water and ethanol.   │
│ 4. Dry the solid in an oven for 24   │
└──────────────────────────────────────┘

```
┌─────────────────────────────────────┐
│       MWCNT-Mag-8-HQ (solid)        │
└─────────────────────────────────────┘
```
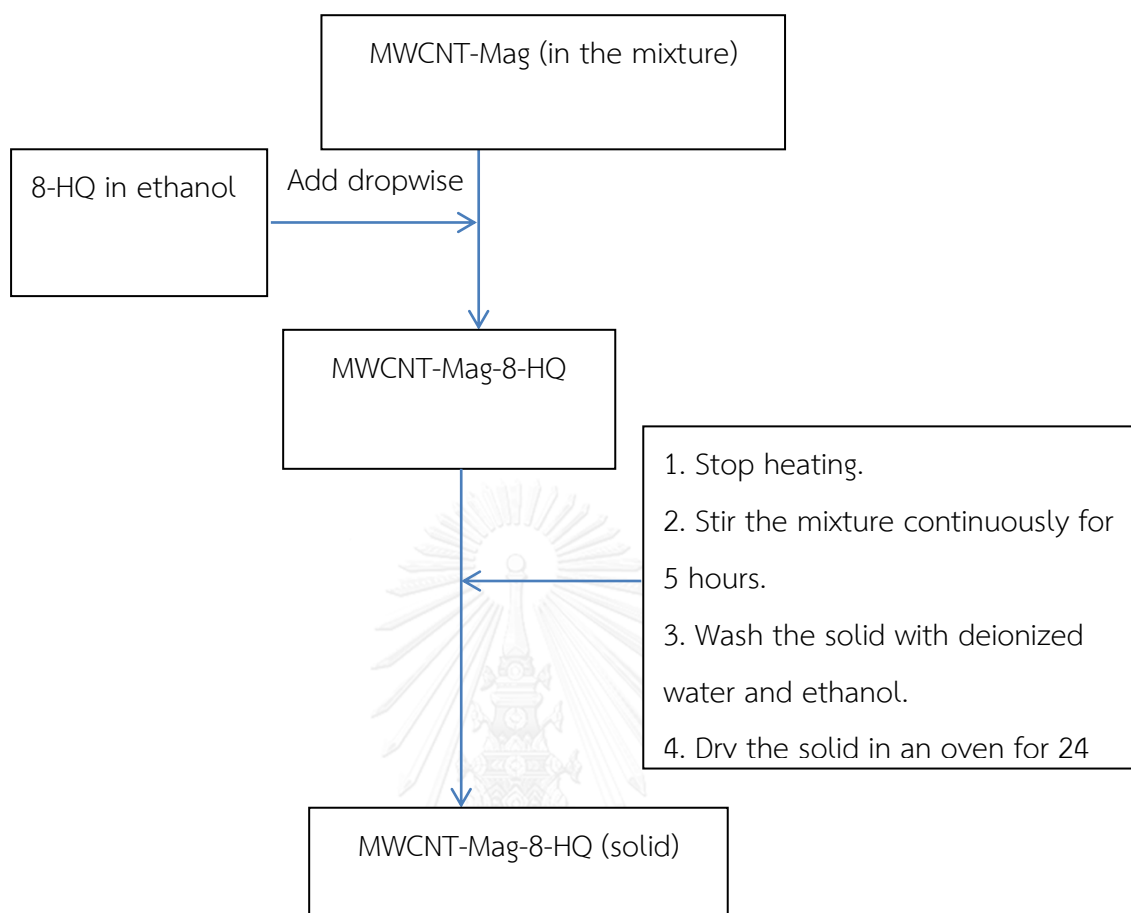
Figure3.2 Procedure of MWCNT-Mag-8-HQ synthesis

3.3 Characterization of the adsorbents

All instruments and technique used for characterization are shown and the condition in the analysis is described in detail in the following part.

3.3.1 Thermogravimetric analysis (TGA)

Thermogravimetric analysis is the technique used to measure the changing in weight of material as a function of temperature (or time). The weight loss was recorded in the temperature range from 50°C to 850°C with heating rate of 10°C/min and nitrogen feed of 20ml/min. The content of 8-HQ in the prepared composites could be calculated from the percentage weight loss.

3.3.2 X-ray diffraction (XRD)

An X-ray diffractometer (, Diffraktometer D8, Bruker AXS) was used to provide important information including the crystallinity of the materials to confirm the structure of MWCNT-Fe$_3$O$_4$. The signal was observed in the 2θ range of 10-80.

3.3.3 Scanning electron microscope (SEM)

A scanning electron microscope (JSM 5800, Jeol) would show the external morphology (texture) of samples by scanning it with a focused beam of electron. The electrons interact with sample's atom and produce the signals of solid samples.

3.3.4 Fourier transform infrared spectroscopy (FT-IR)

Fourier transform infrared spectra of the materials was recorded with Nicolet FT-IR in wavenumber range between 650 cm^{-1} and 4000 cm^{-1} with transmittance mode using attenuated total reflectance (ATR) method. The resulting spectra showed the signal of different molecular bonds, creating a fingerprint of 8-HQ and MWCNT-Mag-8-HQ.

3.3.5 Vibrating sample magnetometer (VSM)

In the analysis by a vibrating sample magnetometer, the sample was placed in a constant magnetic field. If the studied sample has magnetic properties, the constant magnetic field will magnetize the sample by aligning the magnetic domains, or the individual magnetic spins. The magnetic field was then created around the sample, called "the magnetic stray field" that can be detected by set of pick-up coils.

3.3.6. Amount of iron in the magnetic composites

To determine the amount of iron in the magnetic composites, magnetic particles were dissolved out of MWCNT-Mag and MWCNT-Mag-8-HQ prepared by using 20, 25 and 30% wt magnetic particles. Stir the magnetic composites 15 mg in 20ml of 5M nitric acid solutions. After that, the concentration of Fe in the obtained solutions was determined by using FAAS.

The results from FAAS will show in unit of mg/L. Thus, we have to convert mg/L to mg/15 mg adsorbents first by using equation 3.1.

$$\text{mg} = \frac{C_d}{1000} \times V \qquad (3.1)$$

V　　=　　volume of determine iron solution (ml)

C_d　　=　　concentration that detected by FAAS (mg/L)

After that, we will convert mg/ 15mg adsorbent that calculated from equation 3.1 to mg/g adsorbent by using equation 3.2.

$$\frac{mg}{g} = \frac{A \times 1000}{g_i} \qquad (3.2)$$

A　　=　　detected concentration that calculate from equation 3.1

g_i　　=　　initial amount of adsorbent (mg)

3.4 Adsorption study

In the adsorption study, MWCNT-Mag and MWCNT-Mag-8-HQ prepared by using various magnetic nanoparticles amounts (20, 25 and 30%) were used to adsorb Pb(II) or Zn(II) ions in aqueous solutions were used. An amount of 15mg adsorbent was mixed with 30 mL of metal ions solution during a specific period of time. The adsorbent was separated by an external magnetic field. The initial and residual metal ions concentrations were determined by using a flame atomic absorption spectrometer (FAAS). All metal ions solutions were prepared from standard 1000mg/L of Pb(II) and Zn(II). The ionic strength of the metal ions solutions were controlled with 0.01M $NaNO_3$. The experiments were performed in triplicate.

3.4.1 Comparison between MWCNT-Mag and MWCNT-Mag-8-HQ

In this experiment, two groups of adsorbents; MWCNT-Mag and MWCNT-Mag-8-HQ prepared by using various magnetic nanoparticles amounts were compared. To observe the adsorption efficiency of these adsorbents, the batch experiments were performed using solutions containing 20mg/L of Pb(II) or Zn(II). The contact time was 60 min. The solution pH value was 5.

3.4.2 Effect of contact time

The effect of contact time on the adsorption of Pb(II) and Zn(II) onto MWCNT-Mag and MWCNT-Mag-8-HQ was investigated by varying the time of batch process in the range of 0-75 min and solutions pH value was 5.0 ± 0.5. The initial concentration of metal ions (Pb^{2+} and Zn^{2+}) was 20 mg/L.

3.4.3 Effect of solution pH

The solution pH is one of the most influencing parameters affecting adsorption. The effect of pH was investigated in pH range of 3-6. If the solution pH was below 2, magnetic nanoparticles started to dissolve out of the MWCNT composites. On the other hand, if the solution pH was above 6, metal ions in solution would precipitate as metal hydroxide. A sodium hydroxide solution (3M) was used to adjust solutions pH value. The initial concentrations of metal ions (Pb^{2+} and Zn^{2+}) were 20 mg/L and the contact time was fixed at 60 min.

3.4.4 Leaching of magnetic particles during adsorption

The leaching of iron from the composites MWCNT-Mag and MWCNT-Mag-8-HQ into metal ions solutions during the adsorption process was determined at different solution pH values. All experiments were performed under the same condition except the solution pH values. The leaching of iron was observed in solutions having pH values in the range of 3-6. The concentration of iron in Pb(II) or Zn(II) ions solutions after adsorption was determined by FAAS. The leaching amounts of Fe were calculated and compared to the magnetic nanoparticles content in the starting adsorbents.

3.4.5 Adsorption kinetics

To study the rate of adsorption, the experiment was performed as described in topic 3.4.1 at room temperature. All the experimental results were fitted by pseudo-first order kinetics and pseudo-second order kinetics model to describe the adsorption kinetics.

3.5.6 Adsorption isotherms

The adsorption isotherms were studied at room temperature(26 ± 2^oC) by varying metal ions concentrations in solutions from 0 to 30mg/L. The experimental results were fitted by Langmuir and Freundlich adsorption model to describe the adsorption equilibrium and to find the maximum capacity of MWCNT-Mag-8HQ in metal ions adsorption. The contact time was fixed at 60min and the solutions pH value was 5

.

CHAPTER IV

RESULTS AND DISCUSSION

4.1 Synthesis of a composite of multi-walled carbon nanotubes, Fe_3O_4 magnetic particles and 8-hydroxyquinoline

A composite of multi-walled carbon nanotubes and magnetic particles (MWCNT-Mag) was first synthesized by co-precipitation method. Iron (II) sulfate and iron (III) sulfate at molar ratio of 1:2 were used as the starting materials and sodium hydroxide as a precipitant. The obtained product was a black color solid. MWCNT-Mag showed a response to an external magnet as shown in Figure 4.1. Then 8-hydroxyquinone was added to the aqueous mixture of MWCNT-Mag to produce MWCNT-Mag-8-HQ. The final product was a black color solid that can also respond to external magnetic field (Figure 4.1 b). MWCNT-Mag could disperse in aqueous media better than did MWCNT-Mag-8-HQ. In this work, the three proportions of magnetic particles were investigated (i.e. 20, 25 and 30 percent by weight of carbon nanotube)

Table4.1 The amount of iron in the magnetic composites prepared by using different starting Fe(II) and Fe(III) amount

Adsorbent	Amount of Fe in composite (mg/g)
MWCNT20Mag	65.15
MWCNT25Mag	80.03
MWCNT30Mag	96.83
MWCNT20Mag-8-HQ	53.55
MWCNT25Mag-8-HQ	64.16
MWCNT30Mag-8-HQ	70.07
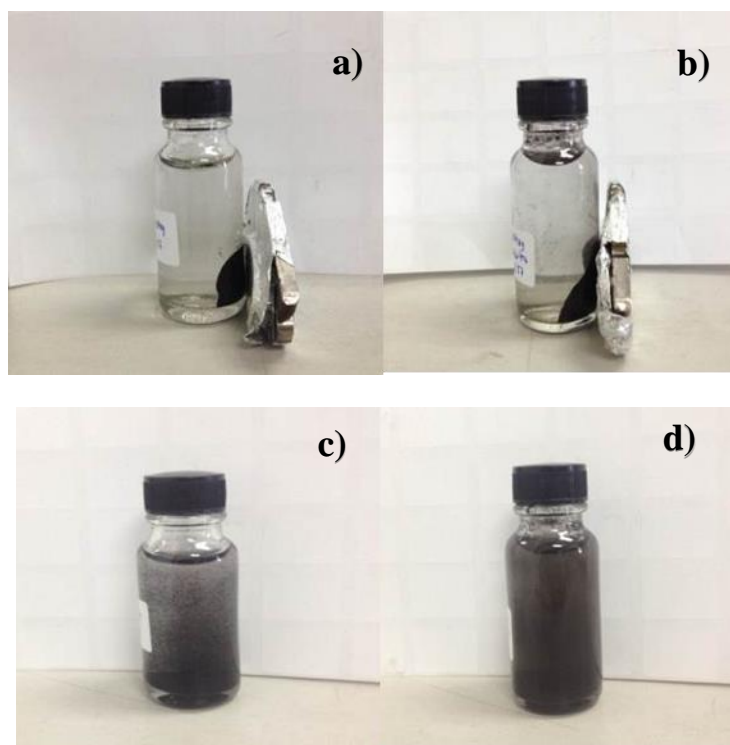
Figure4.1 Response to an external magnet of (a) MWCNT-Mag and (b) MWCNT-Mag-8-HQ. The dispersion of (c) MWCNT-Mag and (d) MWCNT-Mag-8-HQ in aqueous media.

The results of iron amounts on MWCNT-Mag and MWCNT-Mag-8-HQ composites are presented in Table 4.1. The results from table 4.1 show that the amount of iron in magnetic composites increased by increasing the initial Fe(II) and Fe(III) amount used in the preapartion. The materials prepared by using 25 and 30% weight magnetic particle contained high amount of attached magnetic composites in both composites with and without 8-hydroxyquinoline. However, the composites with 8-hydroxyquinoline had less content of magnetic particles when compared with composites that have no 8-hydroxyquinoline due to the shorter time for magnetic particles to precipitate on MWCNT in synthesis process. In the preparation, 8-hydroxyquinoline was added into the mixture of MWCNT and magnetic composites shortly after the precipitation of magnetic particles. Therefore, 8-hydroxyquinoline was likely to compete with magnetic particles in the adsorption onto MWCNT surface.

4.2 Characterization of adsorbents

4.2.1 External morphology of materials

The morphology of the composite of multi-walled carbon nanotubes, magnetic particles and 8-Hydroxyquinoline (MWCNT-25Mag and MWCNT-25Mag-8-HQ) was observed by using a scanning electron microscope (SEM) and the results are shown in Figure 4.2. SEM image of MWCNT-25Mag composite (Figure 4.2 (a)) show the surface that comprise of carbon nanotubes as the base support and magnetic particles spread over their surface (red circle). After adding 8-hydroxyquimoline, the surface of multi-walled carbon nanotubes was covered by 8-hydroxyquimoline and magnetic particles as shown in Figure 4.2 (b) and (c)
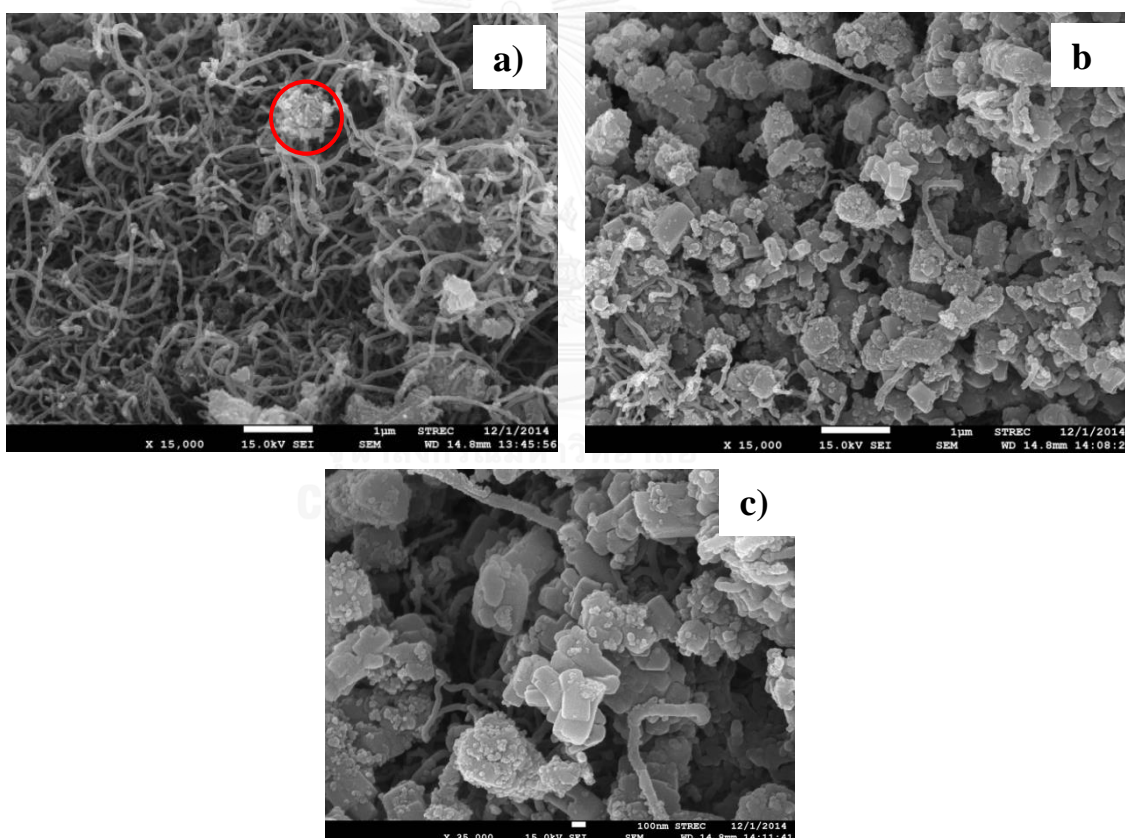
Figure4.2 image of (a) MWCNT- 25Mag, (b) MWCNT-25Mag-8-HQ (x15000) and (c) MWCNT-25Mag-8-HQ (x35000).

4.2.2 Functional groups on the composites

To confirm the successful doping of 8-HQ onto the magnetic composite, Fourier transform infrared spectroscopy (FT-IR) was used. The signal observed in the analysis of the pure 8-HQ and MWCNT-Mag-8-HQ prepared by using various magnetic amounts were compared.

FT-IR spectra of pure 8-HQ and MWCNT-Mag-8-HQ (prepared by using 25% magnetic nanoparticles) were recorded and compared in Figure 4.3. The characteristic bonds and signals were observed as follows. In the spectra of 8-HQ, the signal at $1570cm^{-1}$ could be C=N stretching; $783cm^{-1}$ was benzene rings C-H vibration; $1275cm^{-1}$ was C-OH stretching vibration and benzene ring vibration of 8-HQ was found around $1370cm^{-1}$. The same signals were also detected in the spectra of MWCNT-Mag-8-HQ and this FT-IR result confirm the successful loading of 8-HQ onto magnetic carbon nanotubes composite.

The comparison of FT-IR characteristic between 8-HQ and MWCNT-Mag-8-HQ prepared by using 20, 25 and 30% wt magnetic particles are shown in Figure 4.4.
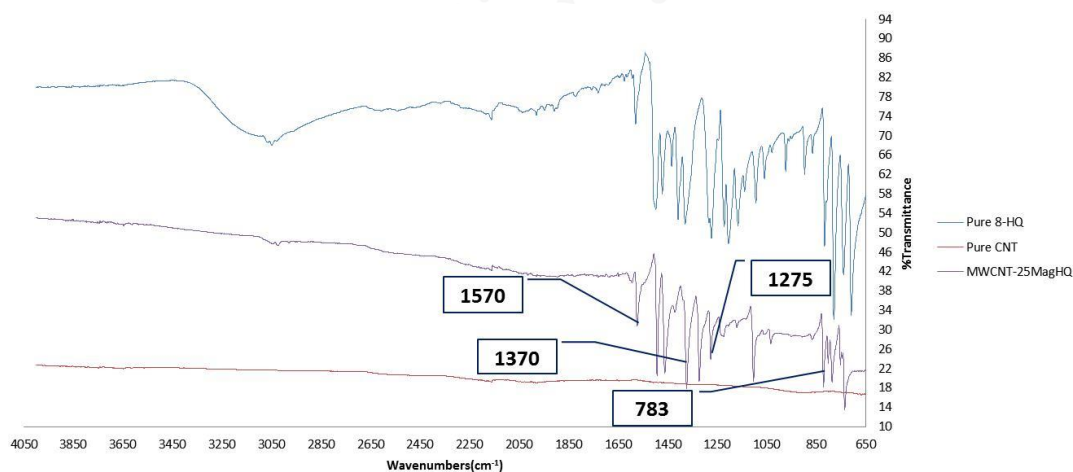
Figure4.3 FT-IR spectra of pure 8-HQ and MWCNT-25Mag-8-HQ and MWCNT
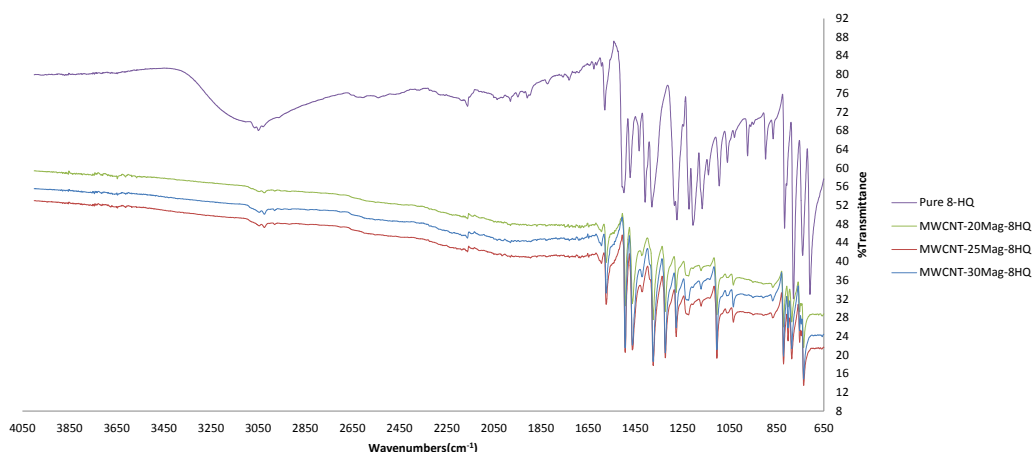
Figure4.4 FT-IR spectra of pure 8-HQ and MWCNT-Mag-8-HQ (prepared by using 20, 25 and 30% magnetic particles)

From the results in Figure 4.4, the IR spectra of MWCNT-Mag-8-HQ prepared by using all studied percent weight of magnetic particles display almost the same patterns. These results indicate that the 8-HQ modified magnetic composites were successfully synthesized.

.

4.2.3 Magnetic properties of the materials

A vibrating sample magnetometer (VSM) was used to detect the magnetization of the adsorbents by placing the sample in a constant magnetic field. According to the results in Table 4.1, the adsorbents prepared with 25 and 30% wt magnetic particles were chosen for the analysis by VSM. The results of the four adsorbents are shown in Figure 4.5.
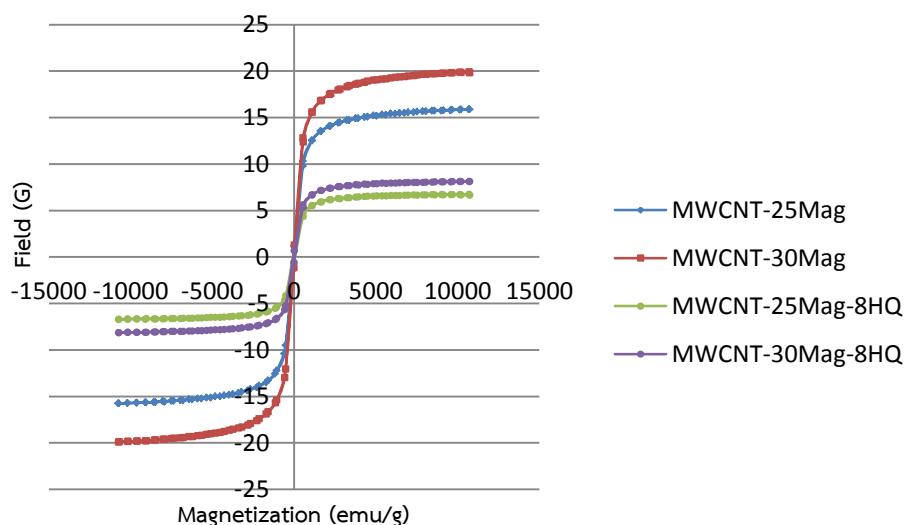
Figure4.5 Magnetization of adsorbents

As shown in Figure 4.5, magnetization results of MWCNT-25Mag and MWCNT-30Mag adsorbents were 15.819 emu/g and 19.907 emu/g, respectively. On the other hand, the magnetization value of MWCNT-25Mag-HQ and MWCNT-30Mag-HQ was 6.736 emu/g and 8.137 emu/g, respectively. The adsorbents with 8-HQ have less amount of iron (Figure 4.1), thus it lead to the decreasing in magnetization of MWCNT-Mag-8-HQ.

The results confirm that the more iron(II) and iron(III) we added in adsorbents, the more magnetization we detected. The values of magnetization of MWCNT-25Mag-8-HQ and MWCNT-30Mag-8-HQ were not much different from each other compared to different dosage of iron(II,III) added. Thus, MWCNT-30Mag-8-HQ seemed to be suitable for this study.

4.2.4 Thermal stability of the materials

Thermogravimetric analysis (TGA) was used to observe the decomposition of the materials when being heated and the weight loss of each composition in the composites was recorded. Due to the difference in decomposition temperature, it indicated the different composition of the materials. MWCNT, MWCNT-Mag and MWCNT-Mag-8-HQ prepared by using 25 and 30% wt

magnetic particles were analyzed by this technique. The results are shown in Figures 4.6-4.9.
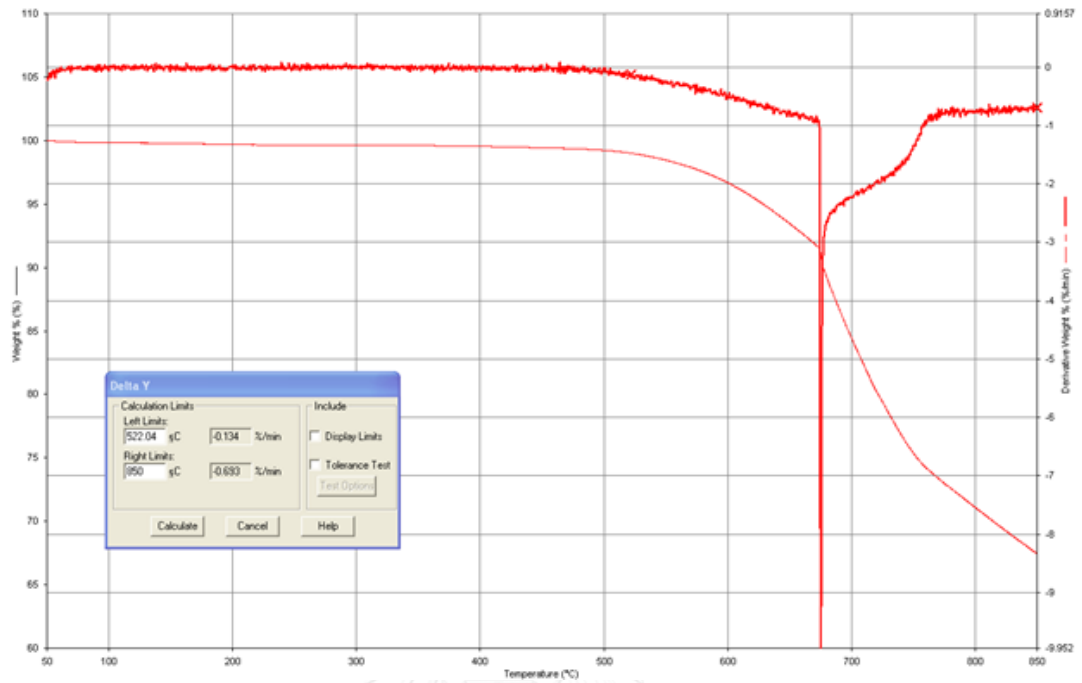
Figure4.6 TGA profile of MWCNT.
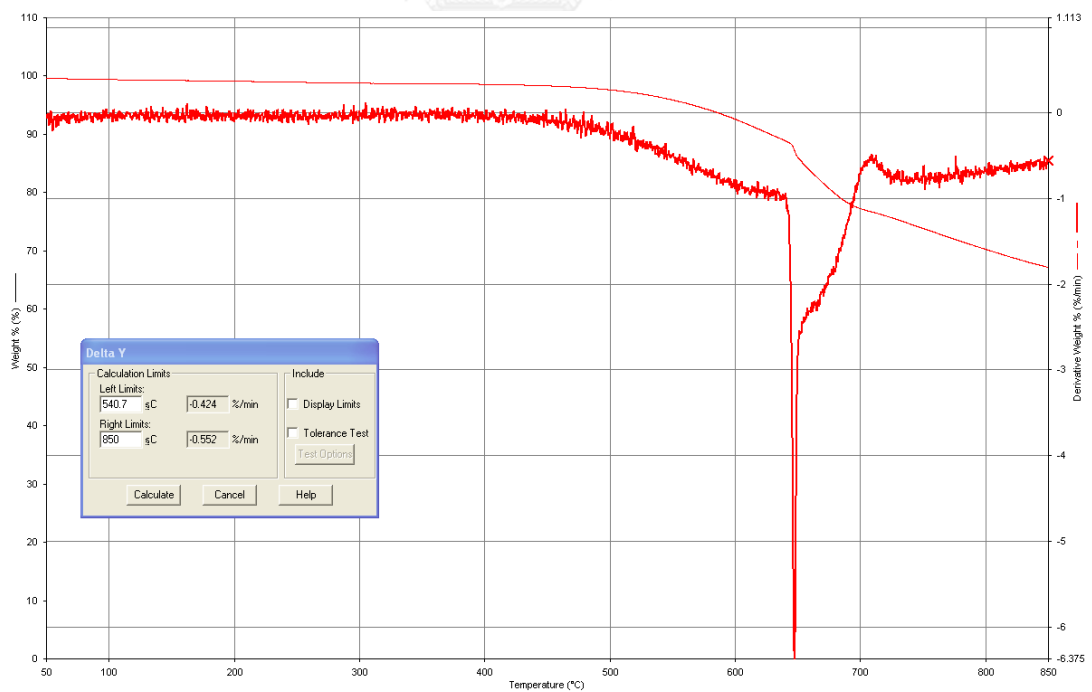
Figure4.7 TGA profile of MWCNT-25Mag.
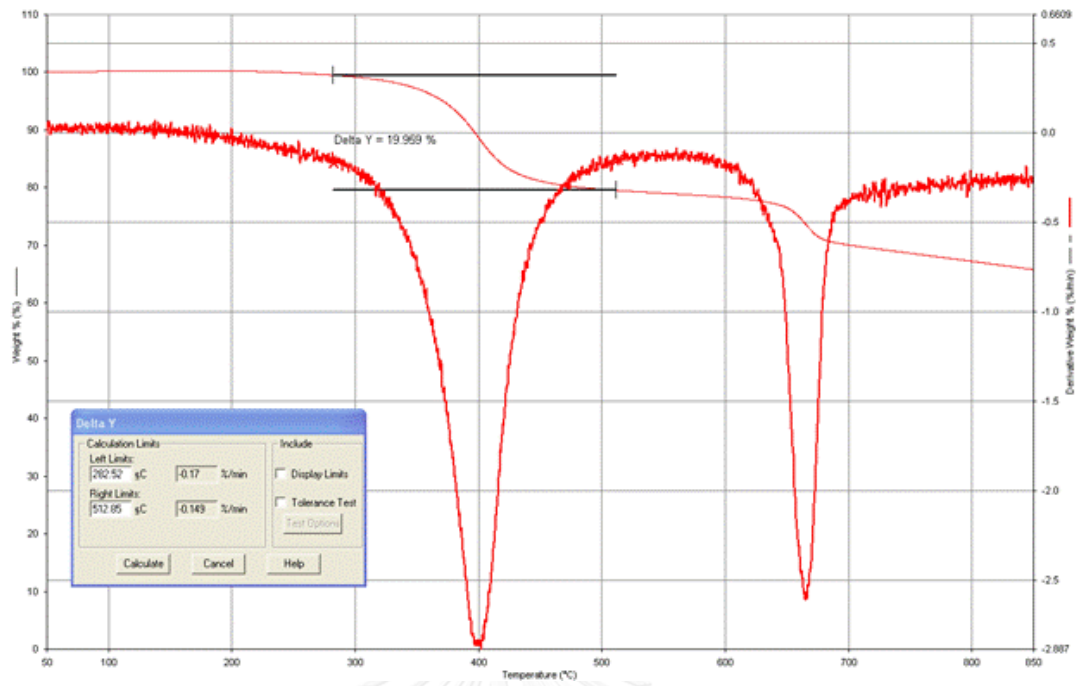
Figure4.8 TGA profile of MWCNT-25Mag-8-HQ
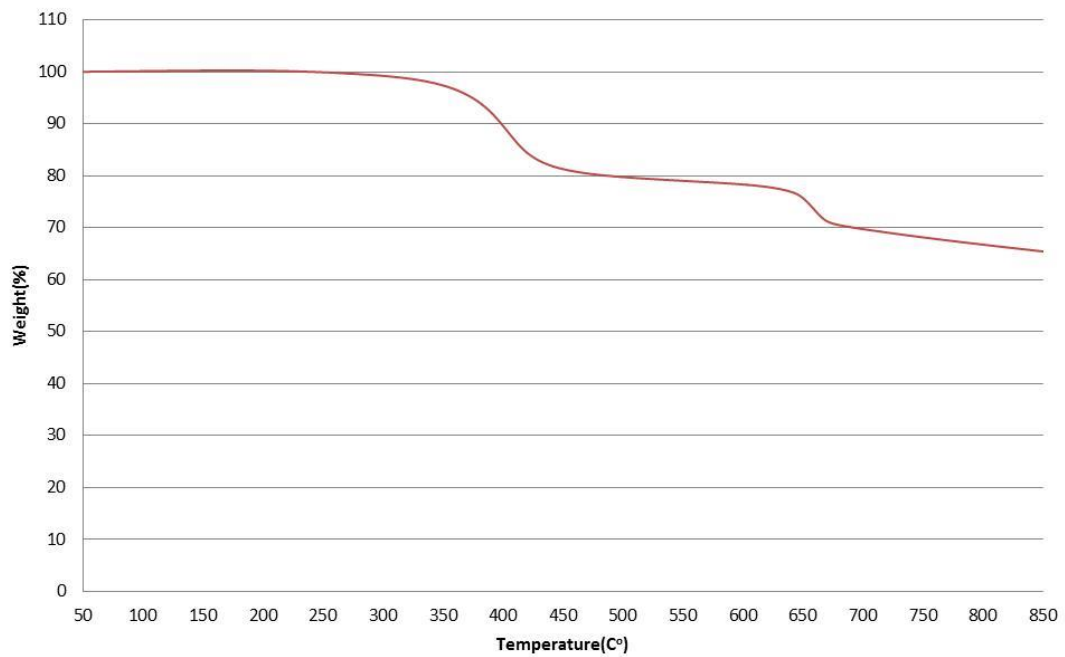
Figure4.9 TGA profile of MWCNT-30Mag-8-HQ

According to the results in Figure 4.6, a weight loss was observed when the temperature rose up to 500°C, which could be attributed to the decomposition of decomposable component of MWCNT at amount of 32% of initial weight. From Figure 4.7, a weight loss was also observed when the temperature rose up to 500°C similar to the MWCNT because magnetic nanoparticles were not decomposed in this range of temperature. Furthermore, a loss of weight in the temperature range of 300-450°C in MWCNT-25Mag-8-HQ and MWCNT-30Mag-8-HQ shown in Figures 4.8 and -4.9 corresponded to the decomposition of 8-HQ in composites and the weight losses of the same extent were observed. These results reveals that the amount of 8-hydroxyquinoline coated on the materials containing different content of magnetic particles was the same.

4.2.5 Results from X-ray diffraction technique (XRD)

This technique was used to confirm the successful deposition of magnetic particles onto carbon nanotube surface. The results from the instrument are shown in Figure 4.10. The XRD pattern of multi-walled carbon nanotube-magnetic particles composite (MWCNT-Mag) was compared to reference database from JCPDS cards #75-0033 (Fe$_3$O$_4$).
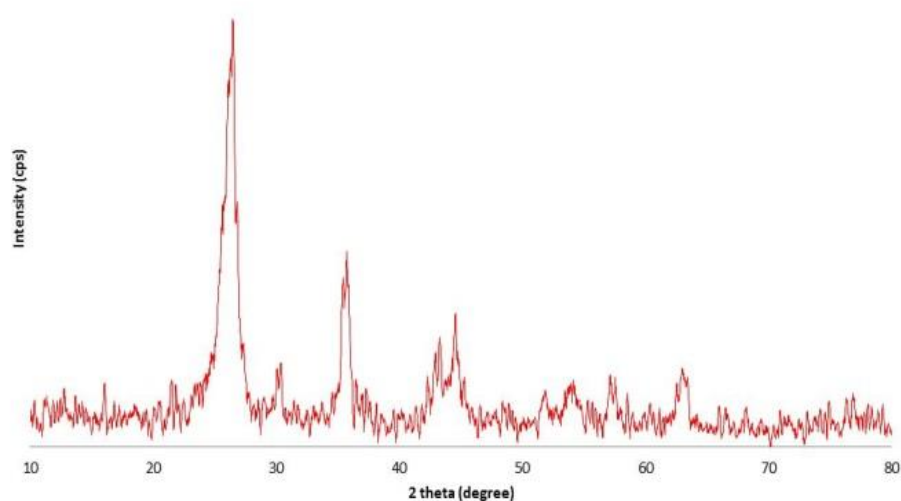
Figure4.10 XRD patterns of MWCNT-25Mag.

From Figure 4.10, the XRD pattern of MWCNT-Mag shows the main diffraction peaks at 2θ of 30.15°, 35.46°, 43.1°, 53.55°, 56.97° and 62.67° that matched well to the reference database of Fe_3O_4. Therefore, the results indicated that the composite contained the magnetic particles.

4.3 Adsorption studies

In the adsorption experiments, MWCNT-Mag and MWCNT-Mag-8-HQ prepared with various contents of magnetic particles were used. To evaluate the efficiency of these adsorbents in metal ions adsorption, the adsorption experiments were designed to be batch experimental. The metal ions solutions contained 20mg/L of Pb(II) or Zn(II). The adsorbent dose of 15 mg was adopted to adsorb metal ions in 30ml solution. The adsorption of metal ions is presented in term of adsorbed amount of the target ions on the adsorbent (mg/g).

4.3.1 Effect of contact time

The time of adsorption to reach their equilibrium was determined in this experiment. The equilibrium time was also used in other experiments. The amount of Zn(II) and Pb(II) ions adsorbed on MWCNT-Mag and MWCNT-Mag-8-HQ at different contact time are shown in Figure 4.11.
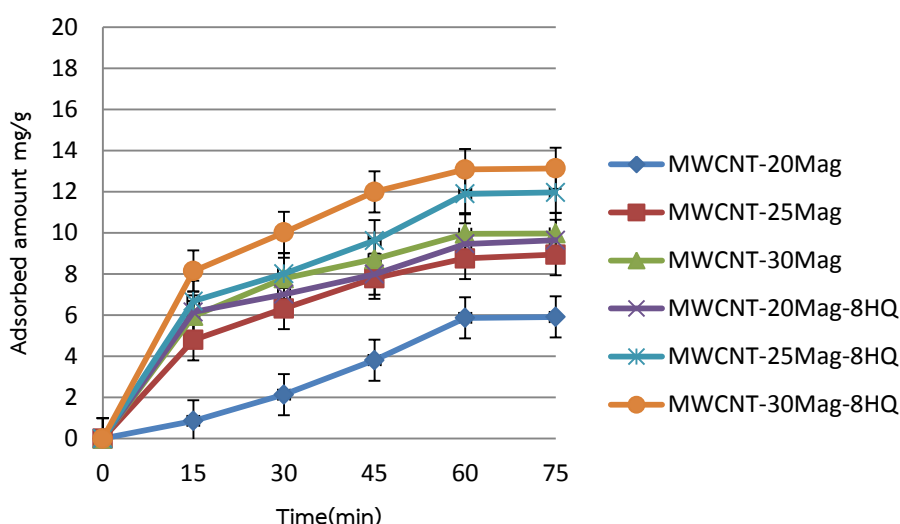
Figure4.11 Effect of contact time on the adsorption of Zn(II) ions by MWCNT-Mag and MWCNT-Mag-8-HQ. (Zn(II) 20mg/L, pH5)

The results show that the efficiency in Zn(II) ions adsorption by all adsorbents increased by increasing the contact time and then reached relatively constant values after 60 minutes of contact time. After 60 minutes, the adsorbed amount did not change despite an increase in contact time. These results indicated that the adsorption equilibrium was attained after 60 minutes. The more magnetic particles we added the more efficiency we gained in adsorption due to higher number of active sites for electrostatic interaction with metal ions in solution. Furthermore, adsorbents doped with 8HQ showed a better efficiency in adsorption than adsorbent without 8-HQ.
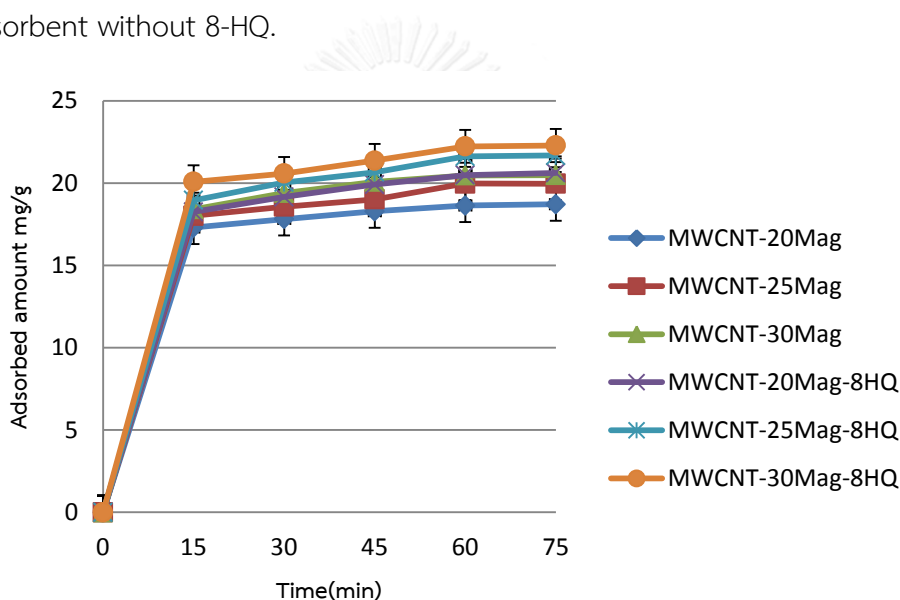
Figure4.12 Effect of contact time on the adsorption of Pb(II) ions by MWCNT-Mag and MWCNT-Mag-8-HQ. (Pb(II) 20mg/L, pH5)

According to the results in Figure 4.12, the adsorption of Pb(II) by all adsorbents increased rapidly at the beginning and gradually reached relatively constant values after 60 minutes of contact time. The adsorption equilibrium under this experimental condition could be attained within 60 minutes. The same trends as observed in Zn(II) adsorption was also found in Pb(II) adsorption. Higher amount of magnetic particles and the presence of 8-HQ in the composite could improve the efficiency of metal ions adsorption.

4.3.2 Effect of solution pH

The pH value could have strong effect on adsorption efficiency of heavy metal ions by adsorbents due to the properties of active sites or charges on the surface of adsorbent would be different at various solution pH values. MWCNT-Mag and MWCNT-Mag-8-HQ were used as adsorbents in this experiment. The solution pH was adjusted to the values in the range of 3-6. In solutions having pH 3 and 4, the iron component was leached from the adsorbents into metal ions solutions during adsorption. The metal ions solutions became yellow due to magnetic particles dissolution. The leaching amount of iron was determined and discussed in detail hereafter. Thus, pH values at 3-4 were not suitable for the use of these adsorbents. At pH value of 6, Pb(II) ions started to precipitate and the white sediment of lead hydroxide was observed. Therefore, the suitable pH value for using these magnetic adsorbents was pH 5. However, these adsorbents could be used in solutions having pH higher than 5 and the metal ions removal would be the results from both adsorption and hydroxide precipitation. In this study, the experiment was performed at pH value of 5. The results of metal ions adsorption (Zn(II) and Pb(II)) at pH 5 are shown in Figure 4.13.
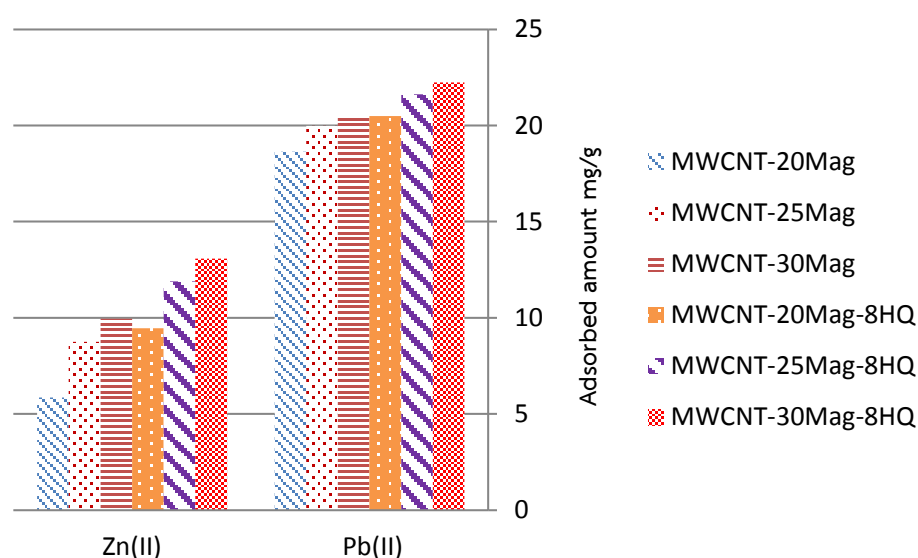
Figure4.13 The adsorption of Zn(II) and Pb(II) ions by MWCNT-Mag and MWCNT-Mag-8-HQ at pH 5 (Pb(II) and Zn(II) 20mg/L, contact time of 60min)

Table4.2 Adsorption capacities at various pH values

Adsorbent	Adsorption capacity (mg/g)					
	pH3		pH4		pH5	
	Zn solution	Pb solution	Zn solution	Pb solution	Zn solution	Pb solution
MWCNT-20Mag	3.86	14.34	5.31	16.23	5.87	18.63
MWCNT-25Mag	4.49	14.53	5.83	16.27	8.75	19.97
MWCNT-30Mag	6.28	14.95	7.55	16.58	10.02	20.46
MWCNT-20Mag-8HQ	6.39	14.95	7.61	16.00	9.46	20.48
MWCNT-25Mag-8HQ	6.87	14.93	8.04	16.02	11.76	21.62
MWCNT-30Mag-8HQ	7.45	14.95	8.53	16.22	13.07	22.23

The results from Figure 4.13 show that the highest efficiency in adsorption of Zn(II) or Pb(II) was achieved when used the composite of MWCNT doped with 30% wt magnetic particles and 8-Hydroxyquinoline. The adsorption may occur through electrostatic interaction between metal ions and negatively charged on MWCNT-Mag surface and complex formation with 8-HQ. From Table 4.2, the charge on the surface of adsorbents should be more negative than positive at pH 5 because the results from experiments at pH below 5 (3-4) gave less efficiency than pH 5. It could conclude that the more pH we use in the experiment the more negative charge on the surface we get. And that's lead to the more adsorption of metal cations take place via electrostatic interaction [35].

4.3.3 Leaching of iron from MWCNT-Mag and MWCNT-Mag-8-HQ

The leaching of iron from MWCNT-Mag and MWCNT-Mag-8-HQ were investigated by measuring the amount of iron that was leached from adsorbents into the metal ions solution having pH in the range of 3 to 5 at fixed operation time. The result was obtained by using FAAS to detect iron component in the solutions. The

amounts of iron leached into the solutions are compared with the initial amount of Fe in the adsorbents as presented in Table 4.3.

Table4.3 Leaching amount of Fe from the composites during adsorption at different pH values

Adsorbent	Initial amount of Fe (mg/g)	Leaching amount (mg/g)					
		pH3		pH4		pH5	
		Zn solution	Pb solution	Zn solution	Pb solution	Zn solution	Pb solution
MWCNT-20Mag	65.15	0.82	0.66	0.57	0.27	0.03	0.01
MWCNT-25Mag	80.03	0.95	0.73	0.78	0.35	0.04	0.06
MWCNT-30Mag	96.83	0.98	0.81	0.81	0.50	0.06	0.06
MWCNT-20Mag-8HQ	53.55	2.43	2.42	1.00	1.23	0.01	0.07
MWCNT-25Mag-8HQ	64.16	2.47	2.57	1.05	1.40	0.01	0.03
MWCNT-30Mag-8HQ	77.07	2.76	2.86	1.05	1.53	0.01	0.07

From Table 4.3, the results showed that at pH value 3 the leaching of Fe in range of 0.83-2.7 mg/g adsorbent was observed in Zn(II) solutions and 0.66-2.86 mg/g adsorbent in Pb(II) solutions. It is clearly seen that the higher solution pH value, the less leaching Fe we detected. At pH value of 5, only a slight leaching of Fe from the adsorbents in Zn and Pb solution was found (less than 0.075 mg/g adsorbent). Thus, the suitable condition for adsorption was at working pH of 5 or higher.

4.3.4 Adsorption Kinetics

The kinetics and the rate of the adsorption process can be described by using pseudo-first order model and pseudo-second order model. The rate law of pseudo-first order model was shown in equation 4.1;

$$\frac{dq_t}{dt} = k_1(q_e - q_t) \tag{4.1}$$

where q_e and q_t are the adsorbed amount of metal ions on the adsorbent (mg/g) at equilibrium and at time t (min). The rate constant of pseudo-first order was k_1 (min^{-1}).

The equation can be integrated with boundary of $t = 0$ to $t = t$ and $q_t = 0$ to $q_t = q_t$. The linear form after integration was written in equation 4.2.

$$\log(q_e - q_t) = \log q_e - k_1 t \tag{4.2}$$

The linear plot between $\log(q_e - q_t)$ and t will give the value of k_1 and q_e from slope and intercept, respectively.

The rate law of pseudo-second order model is shown in equation 4.3;

$$\frac{dq_t}{dt} = k_2(q_e - q_t)^2 \qquad (4.3)$$

where q_e and q_t are the adsorbed amount of metal ions on the adsorbent (mg/g) at equilibrium and at time t (min). The rate constant of pseudo-second order was k_2 (g mg^{-1} min^{-1}).

The equation can be integrated with boundary of $t = 0$ to $t = t$ and $q_t = 0$ to $q_t = q_t$. The linear form after integration is given in equation 4.4.

$$\frac{1}{q_e - q_t} = \frac{1}{q_e} + k_2 t \qquad (4.4)$$

The equation can be rearranged for easy linear plot as shown in equation 4.5.

$$\frac{t}{q_t} = \left(\frac{1}{k_2 q_e^2}\right) + \frac{t}{q_e} \qquad (4.5)$$

The linear plot between $\frac{t}{q_t}$ and t will give the value of k_2 and q_e from intercept and slope, respectively.

In this study, the experiment was performed under a condition of fixed pH value at 5, initial concentration of metal ions (Zn and Pb) of 15 mg/L and the contact time was varied between 0–75 min. MWCNT-30Mag and MWCNT–30Mag-8-HQ were chosen for this investigation. The results are shown in Figures 4.14-4.15.
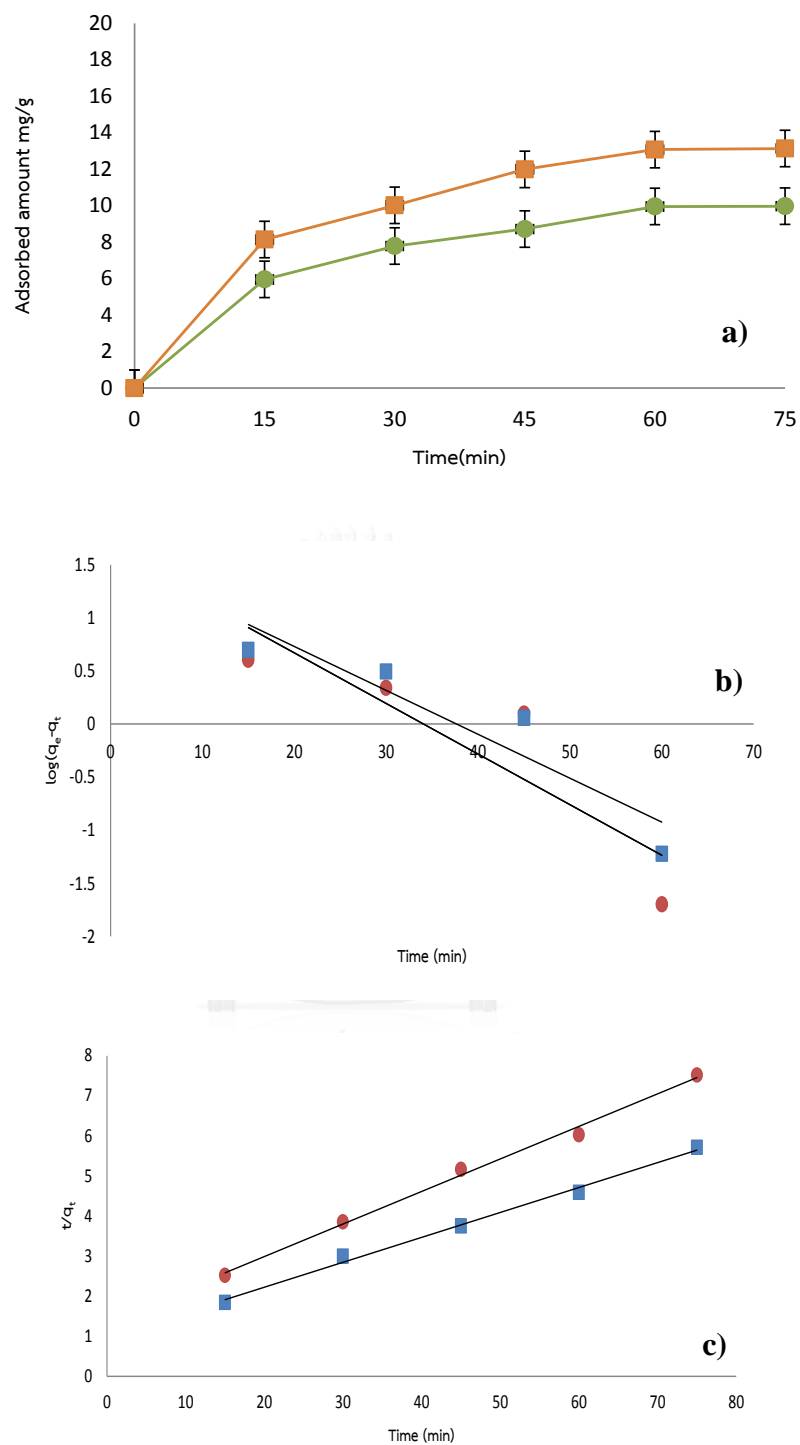
Figure4.14 Experimental data of (a) Zn(II) adsorption at different contact time, (b) pseudo-first-order kinetics plot of Zn(II) adsorption and (c) pseudo-second-order kinetics plot of Zn(II) adsorption. (•)MWCNT-30Mag and (■) MWCNT-30Mag-8-HQ.
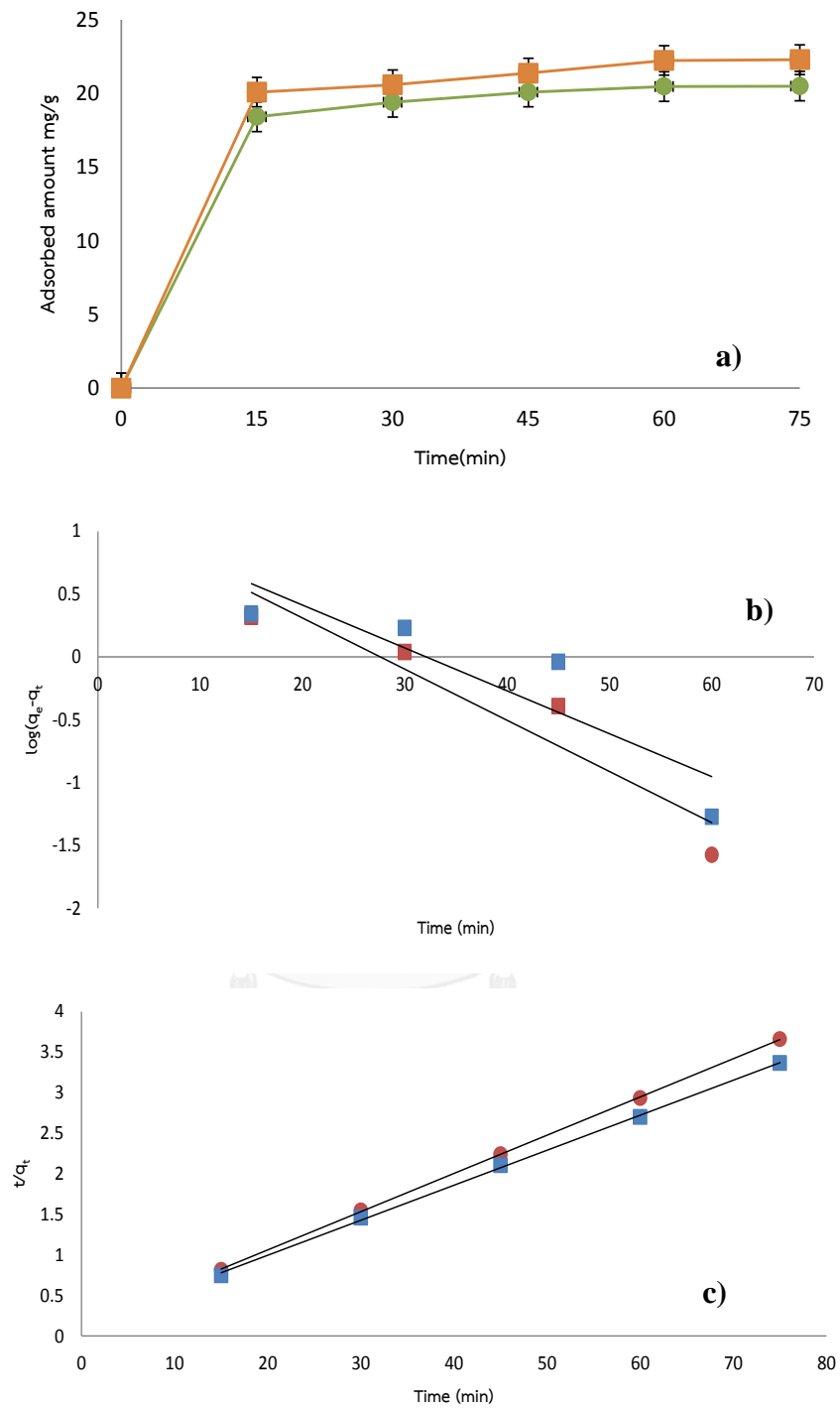
Figure4.15 Experimental data of (a) Pb(II) adsorption at different contact time, (b) pseudo-first-order kinetics plot of Pb(II) adsorption and (c) pseudo-second-order kinetics plot of Pb(II) adsorption. (•) MWCNT-30Mag and (■) MWCNT-30Mag-8-HQ.

From results in Figures 4.14-4.15, all calculated data of pseudo-first order model and pseudo-second order model from linear plot are summarized in Table 4.4.

Table 4.4 Kinetics parameters calculated from kinetics models for the adsorption of Zn(II) and Pb(II) ions onto MWCNT-30Mag and MWCNT-30Mag-8-HQ

Kinetics model	Metal	Adsorbent	$q_{e,exp}$ (mg/g)	$q_{e,cal}$ (mg/g)	rate constant		R^2
					k_1 (min^{-1})	k_2 (min^{-1})	
Pseudo-first order	Zn	MWCNT-30Mag	9.97	5.07	0.048		0.782
		MWCNT-30Mag-8-HQ	13.13	4.74	0.041		0.862
	Pb	MWCNT-30Mag	20.49	3.08	0.041		0.893
		MWCNT-30Mag-8-HQ	22.28	2.99	0.034		0.791
Pseudo-second order	Zn	MWCNT-30Mag	9.97	12.32		0.005	0.995
		MWCNT-30Mag-8-HQ	13.13	16.08		0.004	0.995
	Pb	MWCNT-30Mag	20.49	21.19		0.019	0.999
		MWCNT-30Mag-8-HQ	22.28	23.15		0.014	0.999

The results show that pseudo-second order model fit to the adsorption data better than pseudo-first order, considering the R^2 values that were higher and close to 1. Moreover, q_e value calculated from pseudo-second order linear plot was closer to q_e observed from experimental, indicating a good fitting of the model to the experimental data. The same results were obtained with all adsorbents (MWCNT-30Mag and MWCNT-Mag-8-HQ). With the assumptions of pseudo-second order model, the adsorption could occur as monolayer sorption via both physisorption and chemisorption[38]

For further explanation, physisorption was likely to occur throughelectrostatic interaction between negatively charged active site on adsorbent surface and metal cations. Chemisorption could be attributed to the chelating mechanism between 8-Hydroxyquinoline and metal ions.

4.3.5 Adsorption Isotherms

The adsorption isotherms show the relation between the amount of analyte adsorbed on adsorbent and concentration of analytes in solution at equilibrium. There are two important isotherm models that are widely used to describe the adsorption equilibrium which are Langmuir adsorption isotherm and Freundlich adsorption isotherm.

The Langmuir isotherm model was developed based on the adsorption that took place at specific and homogeneous sites on the adsorbent. The equation is shown in equation 4.6.

$$q_e = \frac{q_m b C_e}{1 + b C_e} \qquad (4.6)$$

The equation 4.6 can be rearranged into linear form as written in equation 4.7;

$$\frac{C_e}{q_e} = \frac{1}{b q_m} + \frac{C_e}{q_m} \qquad (4.7)$$

where q_e = the amount of metal ions adsorbed per unit weight of adsorbent at equilibrium (mg/g)

q_m = maximum adsorption capacity for forming single layer (mg/g)

b = the constant related to the free energy of adsorption (L/mg)

C_e = the equilibrium concentration of the metal ions in the bulk solution (mg/L)

A plot of $\frac{C_e}{q_e}$ versus C_e should give a straight line with intercept of $\frac{1}{b q_m}$ and slope of $\frac{1}{q_m}$.

The Freundlich isotherm model assumed that the adsorption of analytes occurred on heterogeneous surface or on active sites of various affinities. The equation is shown in equation 4.8.

$$q_e = K_f \, C_e^{1/n} \qquad (4.8)$$

The Freundlich isotherm model can be linearized with logarithmic form as follows;

$$logq_e = logK_f + \tfrac{1}{n} logC_e \qquad\qquad (4.9)$$

where K_f = an indicator of adsorption capacity of the adsorbent (mg/g). Higher the maximum capacity, higher value the K_f is obtained

$1/n$ = a measure of intensity of adsorption. Higher the 1/n value, more favorable the adsorption is. Generally, $n < 1, \dfrac{1}{n} > 1$

A plot of log q_e versus log C_e should give a straight line with intercept of log K_f and slope of $\dfrac{1}{n}$.

The adsorption isotherms experiment was performed under the following condition; pH value at 5, contact time of 60 min and , initial concentration of metal ions (Zn and Pb) varied in the range of 1-28 mg/L at 30°C. MWCNT-30 Mag and MWCNT–30Mag-8-HQ were used. The experimental data and adsorption isotherm plots are shown in Figures 4.15-4.16.
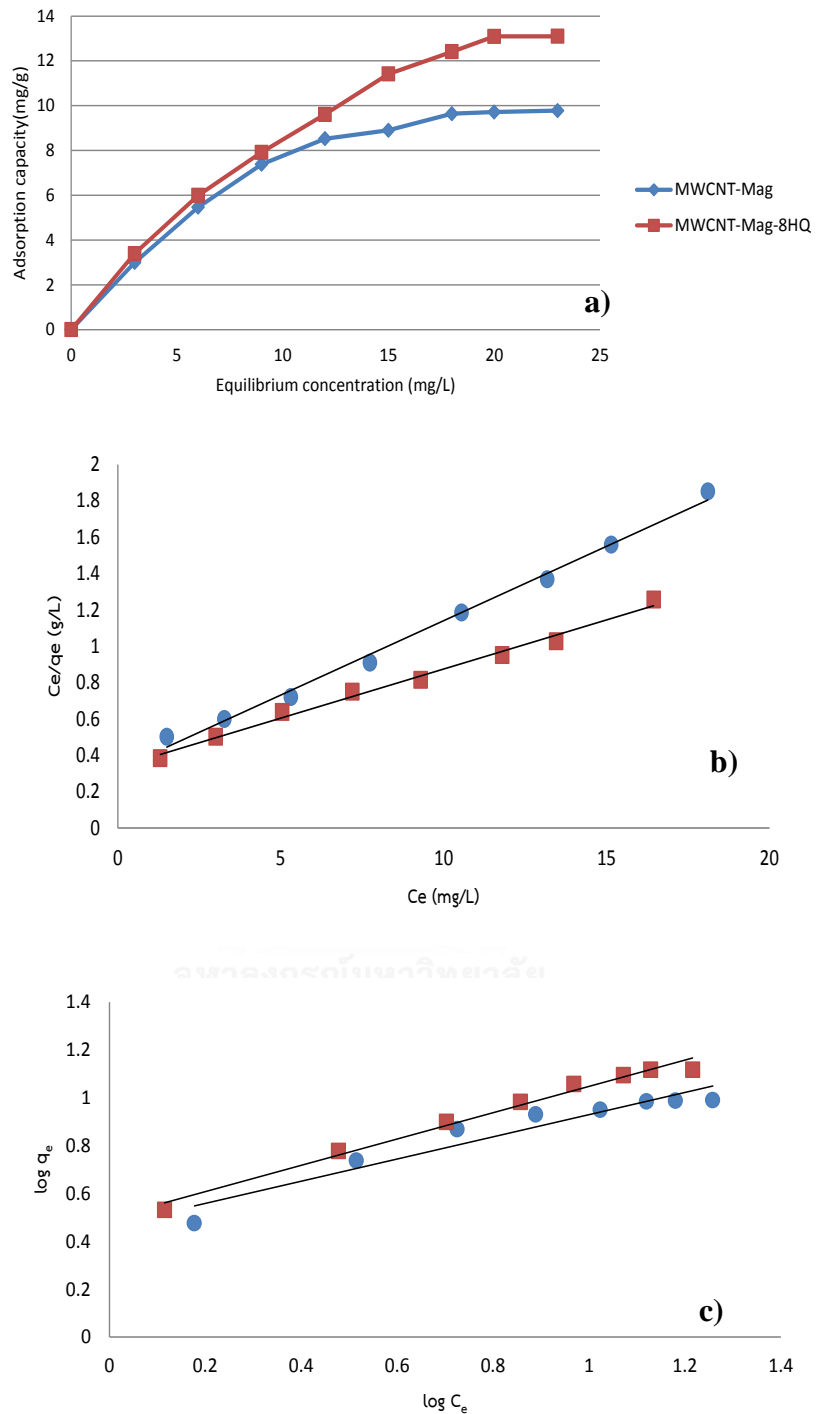
Figure4.16 The plot of (a) Adsorption isotherm of Zn(II), (b) Langmuir isotherm plot for the adsorption of Zn(II) and (c) Freundlich isotherm plot for the adsorption of Zn(II). (•)MWCNT-30Mag and (■)MWCNT-30Mag-8-HQ.
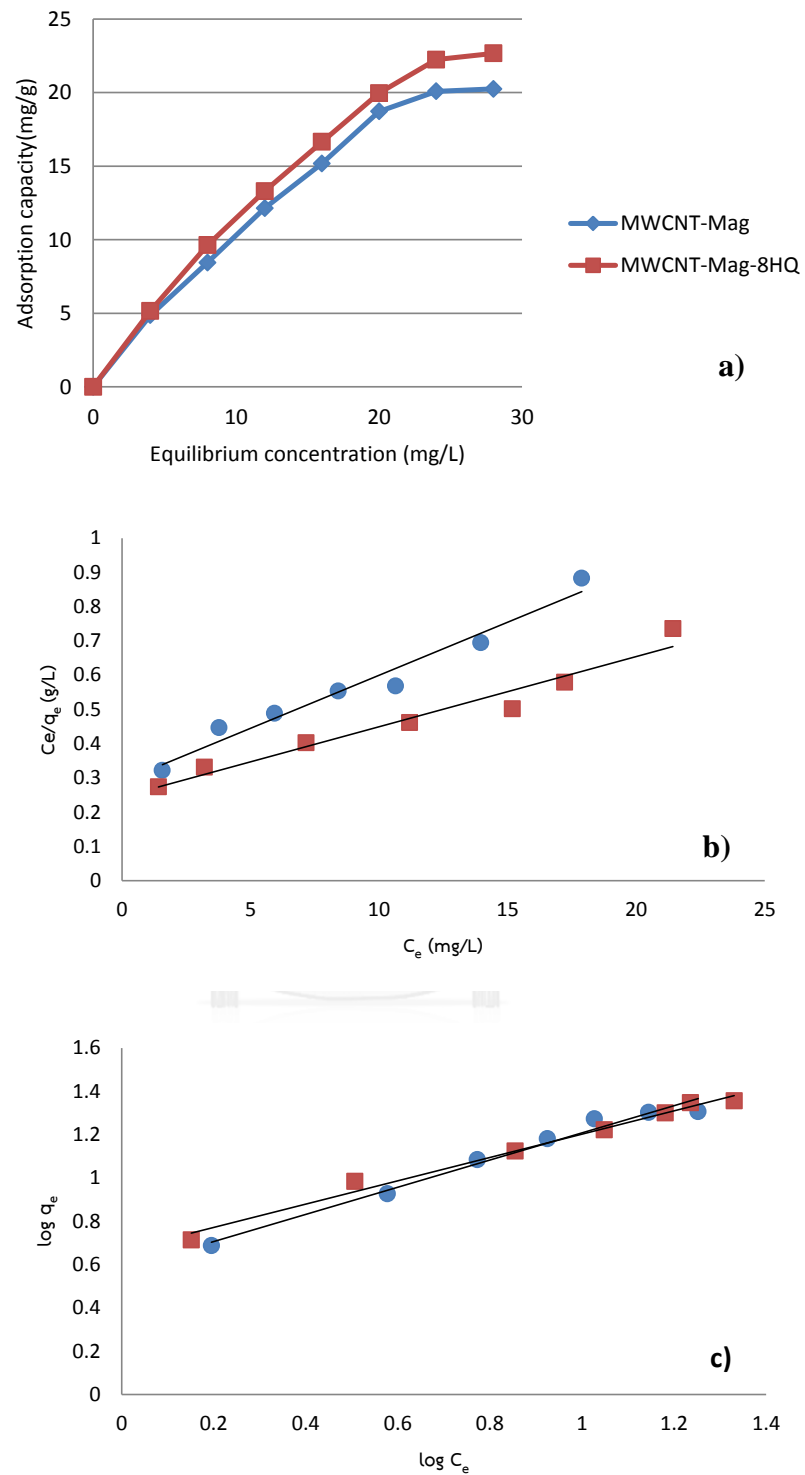
Figure4.17 The plot of (a) Adsorption isotherm of Pb(II), (b) Langmuir isotherm plot for the adsorption of Pb(II) and (c) Freundlich isotherm plot for the adsorption of (c) Pb(II). (•)MWCNT-30Mag and (■)MWCNT-30Mag-8-HQ.

From Figure 4.16-4.17, all the calculated parameters of Langmuir model and Freundlich model are shown in Table 4.5.

Table4.5 Langmuir and Freundlich constants for adsorption of metal ions on MWCNT-Mag and MWCNT-Mag-8-HQ

Adsorbent	Metal	Langmuir constants				Freundlich constants		
		q_m (mg/g)	b (L/mg)	R^2	R_L	K_f	n	R^2
MWCNT-30Mag	Zn	12.22	0.25	0.994	0.146-0.567	1.59	2.16	0.922
	Pb	32.26	0.11	0.964	0.251-0.700	1.79	1.59	0.978
MWCNT-30Mag-8-HQ	Zn	18.52	0.16	0.991	0.212-0.674	1.64	1.82	0.984
	Pb	48.78	0.08	0.955	0.299-0.750	1.94	1.86	0.987

From the results in Table 4.5, both model seemed to fit to the adsorption data considering the value of R^2. However, regarding the nature of adsorbent, the adsorption may be described by the assumption of Freundlich model better than Langmuir model because the adsorbents probably had heterogeneous surface. Thus, by following the assumption of Freundlich model, the adsorption of metal ions on these adsorbents occurred via weak interaction on the surface. The interaction can be occurred in many kinds due to there were many groups on the adsorbent that can adsorb metal ions. These results also support the results observed in adsorption kinetics study.

The metal ions may adsorb onto the surface of MWCNT-Mag and MWCNT-Mag-8-HQ at their active sites following Freundlich model assumption. For MWCNT-Mag, it comprised of heterogeneous active sites which were CNT surface and magnetic particles surface (OH$^-$ sites). Nonetheless, the ones responsible for metal ions adsorption was likely to be magnetic particles site because they could have negative charge on surface that attracted metal cations better than the MWCNT sites did. In the case of MWCNT-Mag-8-HQ, 8-HQ on adsorbents was the main active sites for metal cations and the adsorption may occur through electrostatic interaction with hydroxyl groups from magnetic particles and the chemisorption of metal ions via complexation with donor atoms (oxygen and nitrogen) on 8-HQ. That made MWCNT-

Mag-8-HQ an adsorbent for selective adsorption of metal ions, compared to MWCNT-Mag.

One important parameter of Langmuir isotherm model was R_L value. This value could give the information whether the adsorption process was favorable or not. R_L value was calculated by using equation 4.10;

$$R_L = \frac{1}{1+bC_i} \qquad (4.10)$$

where b = the constant related to the free energy of adsorption (L/mg)

C_i = the initial concentration of metal ions (mg/L)

R_L values indicate the type of isotherms and adsorption equilibrium as summarized in Table 4.6.

Table4.6 R_L value and type of isotherms

R_L Value	Type of isotherm
$R_L > 1$	Unfavorable
$R_L = 1$	Linear
$0 < R_L < 1$	Favorable
$R_L = 0$	Irreversible

Considering the calculated R_L parameters in Table 4.6, it shows that the adsorption process of Zn(II) and Pb(II) were favorable. The maximum adsorption capacity of MWCNT-30Mag in Zn(II) and Pb(II) adsorption were 12.22 and 32.26 mg/g, respectively. For MWCNT-30Mag-8-HQ, the maximum capacity in Zn(II) and Pb(II) adsorption were 18.52 and 48.78 mg/g, respectively.

CHAPTER V

CONCLUSION

The composite of multi-walled carbon nanotubes and magnetic particles (MWCNT-Mag) was synthesized via co-precipitation method. The magnetic composite was further doped with 8-Hydroxyquinoline. The results of materials characterization observed by using a scanning electron microscope, Fourier transform infrared spectroscopy, vibrating sample magnetometer (VSM) and X-ray diffraction technique, confirmed that Fe_3O_4 magnetic particles could be deposited onto multi-walled carbon nanotubes and the composites showed magnetic properties. 8-HQ was successfully doped onto the magnetic composites. The composites could disperse well in water and responded to an external magnetic field. The magnetization value of composites that contain of 8-Hydroxyquinoline decreased by 55-60 % when compared with non-doped magnetic composites.

Both MWCNT-Mag and MWCNT-Mag-8-HQ showed a potential in removal of heavy metal ions from solutions. The adsorption experiment was performed using batch system. When compared the efficiency of the both adsorbents, MWCNT-Mag-8-HQ showed a better efficiency in adsorption of both Zn(II) and Pb(II) ions from aqueous solutions. Furthermore, the suitable conditions of the process were obtained as follows. The contact time to reach the equilibrium was 60 min and working pH was at 5. If the pH value was lower than 5, the magnetic particles in the composites would be dissolved into the solutions. On the other hand, if the pH value was higher than 5, the metal ions in solution would start to precipitate and the removal of metal ions would be the results of both precipitation and adsorption.

The adsorption kinetics of this process followed the pseudo-second order kinetics model for both composites. The adsorption could occur through physisorption and chemisorption. Physisorption was the result of the electrostatic interaction between metal cations and negative adsorbent surface. Chemisorption could occur via chelating mechanism between 8-Hydroxyquinoline and metal ions.

The adsorption isotherms were better fitted by Freundlich model than Langmuir model. Then, the adsorption of metal ions on adsorbent occurred as monolayer coverage on heterogeneous surface. The maximum capacity of MWCNT-30Mag in Zn(II) and Pb(II) adsorption were 12.22 and 32.26 mg/g, respectively. For MWCNT-30Mag-8-HQ, the maximum capacities in Zn(II) and Pb(II) adsorption were 18.52 and 48.78 mg/g, respectively.

REFERENCES

[1]   Al-Ghouti, M.A. and Al-Degs, Y.S. New adsorbents based on microemulsion modified diatomite and activated carbon for removing organic and inorganic pollutants from waste lubricants. <u>Chemical Engineering Journal</u> 173(1) (2011): 115-128.

[2]   Nieto-Delgado, C. and Rangel-Mendez, J.R. Production of activated carbon from organic by-products from the alcoholic beverage industry: Surface area and hardness optimization by using the response surface methodology. <u>Industrial Crops and Products</u> 34(3) (2011): 1528-1537.

[3]   Solisio, C., Lodi, A., Lodi, A., and Borghi, M.D. Removal of exhausted oils by adsorption on mixed Ca and Mg oxides. <u>Water Research</u> 36 (2002): 899–904.

[4]   Ali, S.D., Hussain, S.T., and Gilani, S.R. Synthesis, characterization and magnetic properties of carbon nanotubes decorated with magnetic MIIFe2O4 nanoparticles. <u>Applied Surface Science</u> 271 (2013): 118-124.

[5]   Sameera, I., Bhatia, R., and Prasad, V. Characterization and magnetic response of multiwall carbon nanotubes filled with iron nanoparticles of different aspect ratios. <u>Physica E: Low-dimensional Systems and Nanostructures</u> 52 (2013): 1-7.

[6]   Yan, L., Chang, P.R., Zheng, P., and Ma, X. Characterization of magnetic guar gum-grafted carbon nanotubes and the adsorption of the dyes. <u>Carbohydrate Polymers</u> 87(3) (2012): 1919-1924.

[7]   Ai, L., Huang, H., Chen, Z., Wei, X., and Jiang, J. Activated carbon/$CoFe_2O_4$ composites: Facile synthesis, magnetic performance and their potential application for the removal of malachite green from water. <u>Chemical Engineering Journal</u> 156(2) (2010): 243-249.

[8]   Guan, Y., Jiang, C., Hu, C., and Jia, L. Preparation of multi-walled carbon nanotubes functionalized magnetic particles by sol-gel technology and its application in extraction of estrogens. <u>Talanta</u> 83(2) (2010): 337-43.

[9]   Cerutti, S., Silva, M.F., Gasquez, J.A., Olsina, R.A., and Martinez, L.D. On-line preconcentration/determination of cadmium in drinking water on activated carbon using 8-hydroxyquinoline in a flow injection system coupled to an inductively coupled plasma optical emission spectrometer. Spectrochimica Acta Part B 58 (2003): 43-50.

[10]   Kosa, S.A., Al-Zhrani, G., and Abdel Salam, M. Removal of heavy metals from aqueous solutions by multi-walled carbon nanotubes modified with 8-hydroxyquinoline. Chemical Engineering Journal 181-182 (2012): 159-168.

[11]   Center, N.R. Diamagnetic, Paramagnetic, and Ferromagnetic Materials. [Online]. 2014. Available from: https://www.ndeed.org/EducationResources/CommunityCollege/MagParticle/Physics/MagneticMatls.htm [10 May 2015]

[12]   Champions, S.f. Classifications of Magnetic Materials. [Online]. 2012. Available from: http://www.school-for-champions.com/science/magnetic_materials.htm#.VFsZo_msUwo [10 May 2015]

[13]   magnetism, H.s.g.t. Classes of Magnetic Materials. [Online]. 2014. Available from: http://www.irm.umn.edu/hg2m/hg2m_b/hg2m_b.html [10 May 2015]

[14]   chemistry, C.S.s.a.s. Information of iron (II, III) oxide. [Online]. 2014. Available from: http://www.chemspider.com/Chemical-Structure.17215625.html [5 May 2015]

[15]   Wei, Y., Han, B., Hu, X., Lin, Y., Wang, X., and Deng, X. Synthesis of Fe_3O_4 Nanoparticles and their Magnetic Properties. Procedia Engineering 27 (2012): 632-637.

[16]   Emadi, M., Shams, E. and Amini, M.K. Removal of Zinc from Aqueous Solutions by Magnetite Silica

Core-Shell Nanoparticles. Journal of Chemistry (2013).

[17]   Harraz, F.A. Synthesis and surface properties of magnetite (Fe_3O_4) nanoparticles infiltrated into porous silicon template. Applied Surface Science 287 (2013): 203-210.

[18]   Lin, C.-C. and Ho, J.-M. Structural analysis and catalytic activity of Fe_3O_4 nanoparticles prepared by a facile co-precipitation method in a rotating packed bed. Ceramics International 40(7) (2014): 10275-10282.

[19]   Shen, L., et al. Facile co-precipitation synthesis of shape-controlled magnetite nanoparticles. Ceramics International 40(1) (2014): 1519-1524.

[20]   Kazemzadeh, H., Ataie, A., and Rashchi, F. Synthesis of magnetite nano-particles by reverse coprecipitation. International Journal of Modern Physics 5 (2012): 160–167.

[21]   Wang, B., Wei, Q., and Qu, S. Synthesis and Characterization of Uniform and Crystalline Magnetite Nanoparticles via Oxidation-precipitation and Modified co-precipitation Methods. Int. J. Electrochem. Sci 8 (2013): 3786 – 3793.

[22]   Morel, M., Martínez, F., and Mosquera, E. Synthesis and characterization of magnetite nanoparticles from mineral magnetite. Journal of Magnetism and Magnetic Materials 343 (2013): 76-81.

[23]   Tang, N.J., Zhong, W., Jiang, H.Y., Wu, X.L., Lui, W., and Du, Y.W. Nanostructured magnetite (Fe_3O_4) thin films prepared by sol–gel method. 282 (2004): 92-95.

[24]   Xu, J., et al. Preparation and magnetic properties of magnetite nanoparticles by sol–gel method. Journal of Magnetism and Magnetic Materials 309(2) (2007): 307-311.

[25]   Lu, T., Wang, J., Yin, J., Wang, A., Wang, X., and Zhang, T. Surfactant effects on the microstructures of Fe_3O_4 nanoparticles synthesized by microemulsion method. Colloids and Surfaces A: Physicochemical and Engineering Aspects 436 (2013): 675-683.

[26]   specialist, N.t.c.n. Carbon nanotubes. [Online]. 2015. Available from: http://www.nanocyl.com/jp/CNT-Expertise-Centre/Carbon-Nanotubes [6 May 2015]

[27]   Wikipedia, t.f.e. Carbon nanotubes. [Online]. 2015. Available from: http://en.wikipedia.org/wiki/Carbon_nanotube [6 May 2015]

[28]   Wikipedia, t.f.e. Zinc. [Online]. 2015. Available from: http://en.wikipedia.org/wiki/Zinc [8 May 2015]

[29]   Wikipedia, t.f.e. Lead. [Online]. 2015. Available from:
        http://en.wikipedia.org/wiki/Lead [8 May 2015]

[30]   Agency, U.S.E.P. Development document for final effluent limitations
        guidelines and standards for the Iron and Steel Manufacturing Point Source
        Category. 2002. 1-58.

[31]   Myoung, J.K. and Gyu, H.C. Study on the PV Driven Dehumidifying System with
        Oyster Shell and Thermoelectric Device. Journal of the Korean Society
        of Marine Environment & Safety 18 (2012): 287-293.

[32]   Social, C.L.i. Types of adsorption. [Online]. 2015. Available from:
        https://www.classle.net/book/types-adsorption [6 May 2015]

[33]   Adsorption Equilibria. . 2015(2015).

[34]   Yu, F., et al. Magnetic carbon nanotubes synthesis by Fenton's reagent
        method and their potential application for removal of azo dye from aqueous
        solution. Journal of Colloid and Interface Science 378(1) (2012): 175-183.

[35]   Gong, J.-L., et al. Removal of cationic dyes from aqueous solution using
        magnetic multi-wall carbon nanotube nanocomposite as adsorbent. Journal
        of Hazardous Materials 164(2-3) (2009): 1517-1522.

[36]   El-Latif, M.M.A., Ibrahim, A.M., Amini, M.K. and Hamide, R.R.A. Alumina/Iron
        Oxide Nano Composite for Cadmium Ions Removal from Aqueous Solutions.
        International Journal of Nonferrous Metallurgy 2 (2013): 47-62.

[37]   Gong, J.-L., Wang, B., Zeng, G.-M., Yang, C.-P., Niu, C.-G., and Niu, Q.-Y. Removal
        of cationic dyes from aqueous solution using magnetic multi-wall carbon
        nanotube nanocomposite as adsorbent. Journal of Hazardous Materials 164
        (2009): 1517-1522.

[38]   Social, C.L.i. Types of adsorption [Online]. Available from:
        https://www.classle.net/book/types-adsorption [30 May 2015]

APPENDIX

APPENDIX A

Effect of contact time

Table A1 Effect of contact time on the adsorption of Zn(II) and Pb(II) with MWCNT-20 Mag

Adsorbant	Time (min)	Adsorbed amount of metal ions (mg/g)	
		Zn (II)	Pb (II)
MWCNT-20 Mag	15	0.86 ± 0.13	17.29 ± 0.14
	30	2.13 ± 0.14	17.81 ± 0.04
	45	3.81 ± 0.34	18.29 ± 0.06
	60	5.87 ± 0.26	18.63 ± 0.04
	75	5.91 ± 0.21	18.71 ± 0.08

Mean ± S.D. (N=3)

Table A2 Effect of contact time on the adsorption of Zn(II) and Pb(II) with MWCNT-25 Mag

Adsorbant	Time (min)	Adsorbed amount of metal ions (mg/g)	
		Zn (II)	Pb (II)
MWCNT-25 Mag	15	4.79 ± 0.15	18.01 ± 0.18
	30	6.32 ± 0.14	18.57 ± 0.07
	45	7.79 ± 0.40	19.01 ± 0.04
	60	8.75 ± 0.25	19.97 ± 0.04
	75	8.94 ± 0.25	19.96 ± 0.09

Table A3 Effect of contact time on the adsorption of Zn(II) and Pb(II) with

MWCNT-30 Mag

Adsorbant	Time (min)	Adsorbed amount of metal ions (mg/g)	
		Zn (II)	Pb (II)
MWCNT-30 Mag	15	5.95 ± 0.25	18.41 ± 0.03
	30	7.79 ± 0.35	19.39 ± 0.07
	45	8.72 ± 0.13	20.08 ± 0.06
	60	9.95 ± 0.06	20.46 ± 0.07
	75	9.97 ± 0.25	20.49 ± 0.08

Table A4 Effect of contact time on the adsorption of Zn(II) and Pb(II) with

MWCNT-20 Mag-HQ

Adsorbant	Time (min)	Adsorbed amount of metal ions (mg/g)	
		Zn (II)	Pb (II)
MWCNT-20 Mag-8-HQ	15	6.15 ± 0.18	18.24 ± 0.07
	30	7.01 ± 0.25	19.15 ± 0.07
	45	7.99 ± 0.03	19.91± 0.06
	60	9.46 ± 0.15	20.48 ± 0.10
	75	9.63 ± 0.33	20.61 ± 0.06

Table A5 Effect of contact time on the adsorption of Zn(II) and Pb(II) with

MWCNT-25 Mag-HQ

Adsorbant	Time (min)	Adsorbed amount of metal ions (mg/g)	
		Zn (II)	Pb (II)
MWCNT-25 Mag-8-HQ	15	6.67 ± 0.13	18.95 ± 0.10
	30	8.01 ± 0.14	20.04 ± 0.09
	45	9.62 ± 0.34	20.66 ± 0.11
	60	11.89 ± 0.26	21.62 ± 0.02
	75	11.96 ± 0.09	21.67 ± 0.07

Table A6 Effect of contact time on the adsorption of Zn(II) and Pb(II) with

MWCNT-30 Mag-HQ

Adsorbant	Time (min)	Adsorbed amount of metal ions (mg/g)	
		Zn (II)	Pb (II)
MWCNT-30 Mag-8-HQ	15	8.14 ± 0.36	20.07 ± 0.11
	30	10.02 ± 0.24	20.58 ± 0.03
	45	11.99 ± 0.40	21.37 ± 0.05
	60	13.04 ± 0.09	22.23 ± 0.05
	75	13.13 ± 0.06	22.28 ± 0.09

APPENDIX B

Effect of pH

Table B1 Effect of pH on the adsorption of Zn(II) and Pb(II) with MWCNT-20 Mag

Adsorbant	pH	Adsorbed amount of metal ions (mg/g)	
		Zn (II)	Pb (II)
MWCNT-20 Mag	3	4.86 ± 0.23	15.34 ± 0.22
	4	5.31 ± 0.21	16.23 ± 0.05
	5	5.87 ± 0.26	18.63 ± 0.04
	6	15.21 ± 0.13	P.C.

Mean ± S.D. (N=3)

P.C.=Precipitate

Table B2 Effect of pH on the adsorption of Zn(II) and Pb(II) with MWCNT-25 Mag

Adsorbant	pH	Adsorbed amount of metal ions (mg/g)	
		Zn (II)	Pb (II)
MWCNT-25 Mag	3	5.49 ± 0.19	15.53 ± 0.08
	4	5.83 ± 0.43	16.27 ± 0.12
	5	8.75 ± 0.25	19.97 ± 0.04
	6	16.51 ± 0.07	P.C.

Table B3 Effect of pH on the adsorption of Zn(II) and Pb(II) with MWCNT-30 Mag

Adsorbant	pH	Adsorbed amount of metal ions (mg/g)	
		Zn (II)	Pb (II)
MWCNT-30 Mag	3	7.28 ± 0.11	15.95 ± 0.35
	4	7.55 ± 0.15	16.58 ± 0.47
	5	10.02 ± 0.07	20.46 ± 0.07
	6	17.98 ± 0.22	P.C.

Table B4 Effect of pH on the adsorption of Zn(II) and Pb(II) with MWCNT-20 Mag-HQ

Adsorbant	pH	Adsorbed amount of metal ions (mg/g)	
		Zn (II)	Pb (II)
MWCNT-20 Mag-8-HQ	3	7.39 ± 0.09	15.95 ± 0.04
	4	7.61 ± 0.08	16.00 ± 0.10
	5	9.46 ± 0.42	20.48 ± 0.10
	6	20.87 ± 0.23	P.C.

Table B5 Effect of pH on the adsorption of Zn(II) and Pb(II) with MWCNT-25 Mag-HQ

Adsorbant	pH	Adsorbed amount of metal ions (mg/g)	
		Zn (II)	Pb (II)
MWCNT-25 Mag-8-HQ	3	7.87 ± 0.05	15.93 ± 0.11
	4	8.04 ± 0.09	16.02 ± 0.11
	5	11.76 ± 0.19	21.62 ± 0.02
	6	24.95 ± 0.32	P.C.

Table B6 Effect of pH on the adsorption of Zn(II) and Pb(II) with MWCNT-30 Mag-HQ

Adsorbant	pH	Adsorbed amount of metal ions (mg/g)	
		Zn (II)	Pb (II)
MWCNT-30 Mag-8-HQ	3	8.45 ± 0.13	15.95 ± 0.15
	4	8.53 ± 0.12	16.22 ± 0.07
	5	13.07 ± 0.09	22.23 ± 0.05
	6	32.30 ± 0.23	P.C.

APPENDIX C

Adsorption isotherms

Table C1 The adsorption isotherms of Zn(II) by using MWCNT-30 Mag

Adsorbant	Metal ions	Initial concentration C_i (mg/L)	Equilibrium concentration C_e (mg/L)	Adsorption capacity (mg/g)
MWCNT-30 Mag	Zn	3	1.5 ± 0.06	2.99 ± 0.12
		6	3.27 ± 0.04	5.46 ± 0.07
		9	5.31 ± 0.07	7.38 ± 0.13
		12	7.74 ± 0.06	8.52 ± 0.12
		15	10.55 ± 0.07	8.9 ± 0.15
		18	13.18 ± 0.05	9.64 ± 0.09
		20	15.14 ± 0.03	9.71 ± 0.06
		23	18.11 ± 0.02	9.78 ± 0.04

Mean ± S.D. (N=3)

Table C2 The adsorption isotherms of Zn(II) by using MWCNT-30 Mag-HQ

Adsorbant	Metal ions	Initial concentration C_i (mg/L)	Equilibrium concentration C_e (mg/L)	Adsorption capacity (mg/g)
MWCNT-30 Mag-8-HQ	Zn	3	1.30 ± 0.07	3.39 ± 0.13
		6	3.00 ± 0.02	5.99 ± 0.03
		9	5.04 ± 0.04	7.91 ± 0.08
		12	7.20 ± 0.02	9.61 ± 0.03
		15	9.29 ± 0.04	11.41 ± 0.08
		18	11.80 ± 0.02	12.41 ± 0.03
		20	13.45 ± 0.03	13.09 ± 0.06
		23	16.45 ± 0.05	13.10 ± 0.10

Table C3 The adsorption isotherms of Pb(II) by using MWCNT-30 Mag

Adsorbant	Metal ions	Initial concentration C_i (mg/L)	Equilibrium concentration C_e (mg/L)	Adsorption capacity (mg/g)
MWCNT-30 Mag	Pb	4	1.57 ± 0.05	4.87 ± 0.10
		8	3.78 ± 0.07	8.45 ± 0.15
		12	5.93 ± 0.05	12.14 ± 0.10
		16	8.41 ± 0.08	15.18 ± 0.16
		20	10.64 ± 0.04	18.71 ± 0.08
		24	13.96 ± 0.03	20.09 ± 0.07
		28	17.88 ± 0.02	20.24 ± 0.03

Table C4 The adsorption isotherms of Pb(II) by using MWCNT-30 Mag-HQ

Adsorbant	Metal ions	Initial concentration C_i (mg/L)	Equilibrium concentration C_e (mg/L)	Adsorption capacity (mg/g)
MWCNT-30 Mag-8-HQ	Pb	4	1.42 ± 0.03	5.17 ± 0.06
		8	3.21 ± 0.02	9.63 ± 0.04
		12	7.16 ± 0.09	13.30 ± 0.19
		16	11.19 ± 0.02	16.65 ± 0.05
		20	15.19 ± 0.02	19.96 ± 0.04
		24	17.22 ± 0.02	22.23 ± 0.04
		28	21.43 ± 0.07	22.66 ± 0.15

VITA

Mr. Pheerakit Thanapitak was born on October 25, 1988 in Bangkok, Thailand. He graduated with a Bechelor of Science degree from Chulalongkorn University in 2011. After that, he has been a graduate student at the Department of Petrochemical and Polymer Science, Chulalongkorn University and become a member of Environmental Analysis Research Unit. He finished his Master's degree of Science in 2014.